NOTES ON RELATIVE PERMEABILITY RELATIONSHIPS

M.B. STANDING, Ph.D.

B-53

TABLE OF CONTENTS

PREFACE

One important function of reservoir and production engineers is to predict results of simultaneous flow of gases and liquids through reservoir rocks. Rates of flow into or away from wells and the fraction of oil and gas that will be recovered are two very important items that the engineer is often required to evaluate. One means of making such predictions is by use of valid engineering equations and specific data on the reservoir fluids and rocks involved.

Relative permeability values are called for in both flow and recovery calculations. In many instances the relative permeability - saturation curve, or equation, selected to represent the reservoir system has more effect on the ultimate answer than any other variable in the calculation. Consequently, it is important that the engineer have a good understanding of relative permeability behavior and be able to select the most appropriate values for use in his calculations.

I believe most engineers have the greatest confidence in their predictions when they have laboratory-measured relative permeability values to use in their calculations. (Yet, in my opinion, laboratory measured values may not always reflect in-situ reservoir behavior.) But laboratory measured values often (usually ?) are not available. So what other sources of data are there ? Basically, there are these:

1. Guess. Take a piece of graph paper and draw curved lines that simulate the shapes seen in text books, technical articles, etc. The accuracy of the resulting relative permeability values in representing your specific reservoir condition will be unknown, but generally poor. Furthermore, other engineers will always argue with the way the curves were drawn.

2. Analogy. Select relative permeability - saturation curves from the petroleum literature and assume that your system has the same characteristics. A very favorite correlation of many engineers is that of Arps and Roberts (Trans.,AIME (1955), 204 ,120) that is

reproduced on pages 386-387 of Craft and Hawkin text " Applied Petroleum Reservoir Engineering ". Results of this approach will be just about as inaccurate as those mentioned above, but will be more acceptable to other engineers.

3. Use measured capillary pressure - saturation data to characterize pore structure of the reservoir rock. Use this characteristic in empirical relationships that relate relative permeability to pore structure as well as saturation and saturation history. In many instances this approach will yield fairly accurate results , as judged by comparison with measured laboratory values. But of equal importance to some calculations, the empirical relationships can often be used to extrapolate and average measured data in a consistant manner.

The subject of these notes is the theory behind the empirical relationships that tie relative permeability to rock pore structure , saturation , and saturation history and the equations that result from the theory. I have found such equations to be very useful in day-to-day engineering calculations - particularly when measured data are limited in extent or non existant but also in judging the validity of measured data. In addition, I feel that developing an understanding of the theory behind these relationships greatly improves one's capability of handling and using relative permeability data.

M.B.Standing
Trondheim, Norway
August 1974
Revised, 1978

NOTES ON RELATIVE PERMEABILITY RELATIONSHIPS

All equations used to calculate fluid flow in reservoir rocks require effective permeability values. The effective permeability expresses the permeability to the fluid flowing under the saturation condition existing in the rock. Effective permeabilities have the units of darcys or millidarcys. The symbols k_g , k_o , and k_w are used to designate effective permeability to gas, oil, and water. In a general sense, effective permeabilities can be considered functions of:

1. pore size distribution
2. wettability
3. saturation
4. saturation history

The absolute permeability of a rock, k , is defined as the permeability to a 100% saturating fluid that does not "react" with mineral components of the rock. In effect, absolute permeability depends only on the first parameter listed above.

Relative permeabilities, k_{rg}, k_{ro}, and k_{rw}, are the result of expressing the effective permeability as a fraction of some base permeability value. The three most common base permeability values used are: (1) the absolute permeability, k , (2) the dry air permeability, k_a, measured at near atmospheric pressure, and (3) the effective permeability of one of the hydrocarbon phases at irreducible water saturation, S_{iw}. Other base permeability values can be used as the term relative is completely general. The above three base permeabilities are numerically different so that the value of the relative permeability may vary depending on which base is being used. For example, consider a core sample that has an absolute permeability of 100 md and, at some particular saturation condition, an effective oil permeability of 50 md. The relative oil permeability at this condition would be

$$k_{ro} = \frac{k_o \,]_{S_o, S_w}}{k} = \frac{50}{100} = 0.50$$

This same core would have an air permeability of about 115 md. The relative oil permeability based on the air permeability would be:

$$k_{ro} = \frac{k_o \,]_{S_o, S_w}}{k_a} = \frac{50}{115} = 0.43$$

If the irreducible water saturation of this core was 30%, the oil permeability at irreducible water saturation and zero gas saturation would be about 0.7 of the absolute permeability. The resulting relative permeability on this base would be:

$$k_{ro} = \frac{k_o \,]_{S_o, S_w}}{k_o \,]_{S_{iw}}} = \frac{50}{70} = 0.71$$

As can be seen from the above example, it is important to know which base permeability is being used in expressing the relative permeability value. Other things being equal, it is usually best to work on an absolute permeability base.

When dealing with relative permeability ratios such as k_{rg}/k_{ro} and k_{rw}/k_{ro}, it is necessary, of course, that both relative permeability values be relative to the same base permeability.

Saturation history is indicated by two terms: drainage and imbibition. Drainage relative permeability curves, or values, apply to processes in which the wetting phase is, or has been, decreasing in magnitude. Imbibition relative permeability curves, or values, apply to processes in which the wetting phase is, or has been, increasing in magnitude. The way of indicating drainage and imbibition relative permeability values is by means of subscripts. That is:

$k_{ro:dr}$ = drainage $\qquad$ $k_{ro:imb}$ = imbibition

Arrows are used on graphs pointing in the direction of wetting phase saturation change to indicate drainage and imbibition curves as shown below.

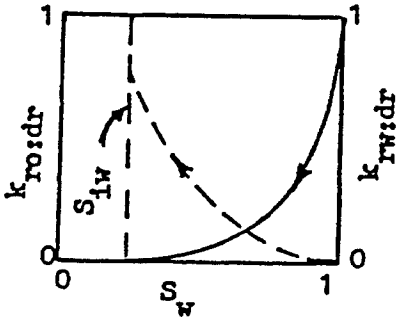

Figure 1a

---oil
——water

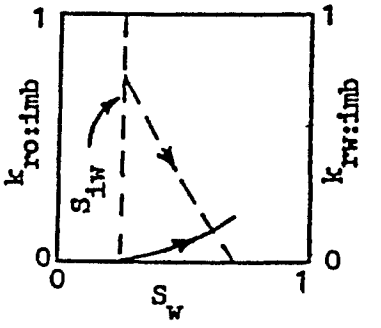

Figure 1b

Figure 1a illustrates drainage oil and water relative permeability curves (absolute permeability base), while Fig. 1b illustrates imbibition curves. Water is the wetting phase in both sets of curves. Figures 2a and 2b illustrate gas and oil relative permeability curves in the presence of irreducible water. S_{iw} denotes the irreducible water saturation value. Of the three phases indicated on the plots, water is considered to have the strongest affinity for the rock surface, (most wetting) followed by oil and gas. Thus, wetting phase saturation values plotted on the abcissa are sums of water and oil saturation values and are indicated by the symbol S_L (total liquid saturation). The arrows point the direction of oil saturation change.

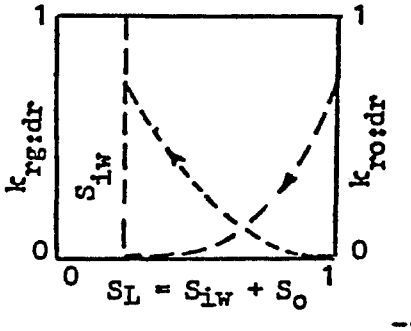

Figure 2a

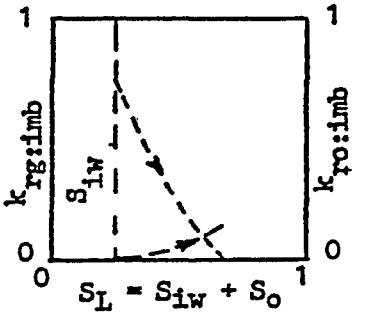

Figure 2b

----- gas
— — — oil

Use of drainage and imbibition relative permeability values in reservoir engineering calculations are usually as follows:

Drainage Curves	Imbibition Curves
1. Tarner or Muskat solution gas drive calculations (gas displaces oil)	1. Water flood calculations (water displaces oil and/or gas)
2. Gravity drainage calculations (gas replaces drained oil)	2. Water influx calculations (water displaces oil and/or gas)
3. Gas drive calculations (gas displaces oil and/or water)	3. Oil displaces gas, water saturation constant (oil being forced into a gas cap)
4. Oil or gas displacing water	

The above is predicated on water being the preferred wetting phase (water-wet rock) and oil being the wetting phase of the two hydrocarbon phases.

Fundamental Concepts About Fluid Distribution in Porous Rocks and Its Effect on Relative Permeability Curves

The purpose of this section is to lay out some simple concepts about the distribution of fluids in porous rocks and the resulting effect on the relative permeability curves.

As a start, it is helpful to consider the pore structure of reservoir rock to be like an assemblage of many different size and different shape pores with each pore interconnecting several other pores. Figure 3 uses the network model of porous media idea proposed by Fatt (1) to illustrate this point. An individual pore is represented by a line segment between connecting points. Keep in mind, though, that each pore has its own size, shape, and surface characteristics. The main point here is there are many different routes by which fluids may get from one part of the system to another part.

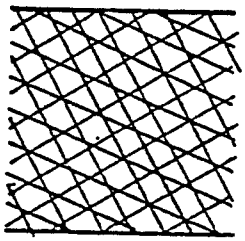

Figure 3

The second concept concerns the distribution of fluids in the pore structure when a particular saturation condition has been reached via a specific desaturation process. Figure 4 shows a hypothetical frequency distribution curve of a pore network such as that illustrated in Fig. 3 and the location of wetting phase (water) and nonwetting phase (oil) in the pore structure when oil has displaced water under capillary control. Under this drainage process, oil enters the largest pores first and progressively desaturated smaller and smaller pores. Some water remains in the oil-invaded pore sizes but it is immobile as a result of being trapped in individual pores by oil or adsorbed on mineral surfaces of the pore walls. In essence, saturation and wettability conditions pretty much determine the pore sizes in which wetting and nonwetting fluid are located. As we shall see later,

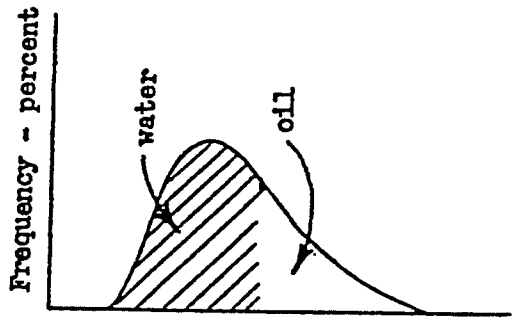

Figure 4

---

* Just how the equivalent pore radius is defined is not important to the present discussion ; that is, we are not concerned here whether the pore cross sections are circular, elliptical, rectangular, etc.

this "location effect" has a lot to do with the way relative permeability varies with saturation.

The third concept that helps to understand relative permeability - saturation behavior deals with flow paths that develop through the rock as a result of saturation changes. If we consider the network model shown in Fig. 3 to be 100% saturated with water (wetting phase), a permeability measurement made with water would yield the absolute value. Water would flow in all pores. This absolute permeability value can be considered to be proportional to some function of the cross-section area of all pores and inversely proportional to some other function of the average flow path length. Note that the network has, in effect, a built-in tortuosity in that the average flow path length is greater than the straight line left-to-right distance.

As mentioned previously, when oil or any other nonwetting phase invades the pore structure, it preferentially enters the largest size pores. This results in a reduced water permeability because the cross-sectional area of the pores conducting water is less than before and the average flow path length of these pores is greater; that is, the water must now flow around pores filled with oil. It is the combined effect of area change and effective flow path length change (as saturation changes) that causes a relative permeability - saturation curve to have a given shape. As illustrated in Fig. 1a, the water curve reduces quite rapidly at first but eventially approaches zero asymptotically and becomes zero at the irreducible water saturation value, S_{iw} .

Changes in flow area and flow path length resulting from saturation changes also combine to yield the drainage oil (nonwetting phase) relative permeability - saturation curve. Note, however (Fig. 1a), that the oil curve terminates at the S_{iw} saturation value at less than full absolute permeability. This is to be expected as there is still some water in the pore structure to impede the flow of oil.

More complex flow behavior occurs when three phases are distributed in the pore structure. Figure 5 presents a concept of phase location when gas, oil, and water are present, but the water saturation is at the irreducible value. The irreducible water resides primarily in the smallest pores, gas is primarily in the largest pores, and oil fills the pore sizes left over. The resulting gas and oil curves are like those illustrated in

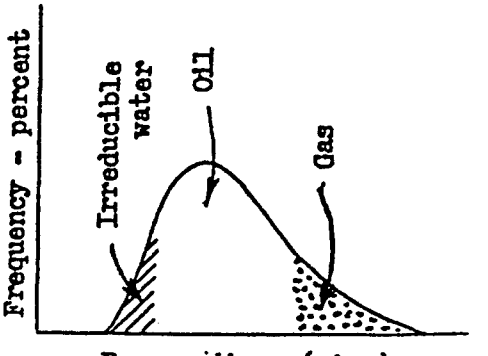

Figure 5

Fig. 2a. The water relative permeability value is zero, of course, because at irreducible saturation value all water is immobile.

The following points summarize the concepts about drainage relative permeability - saturation behavior presented so far. Imbibition curve concepts and behavior will be presented later.

1. Each fluid moves through separate groups of connected pores. Two or three fluids do not flow in the same pore. Saturation changes cause redistributions of the pore size occupied by the separate fluids.

2. The shape of relative permeability - saturation curves comes about from changes of flow area and flow path length as saturations change. The area changes are tied into the pore size distribution of the rock.

3. In water wet systems in which water and hydrocarbon phases have become distributed under capillary control, water preferentially fills the smallest pores, gas fills the largest pores, and oil fills an intermediate range of pore sizes that depend on the water and gas saturation values. As a consequence of this distribution ;

   a) k_{rw} depends only on the amount of mobile water, $(S_w - S_{iw})$, present. It does not depend on whether the hydrocarbon phase is oil, gas, or both.

   b) k_{rg} depends on the amount of gas present, S_g. It does not depend on whether the other phases are water, oil, or both.

   c) k_{ro} depends on the amount of oil present, S_o , and the range of pore size in which it lies. k_{ro} for $S_o = 0.55$, $S_w = 0.40$, $S_g = 0.05$ will be greater than for saturation values of $S_o = 0.55$, $S_w = 0.30$, $S_g = 0.15$ because oil will be distributed in smaller pores in the second case. It is necessary to specify two saturation values when defining oil relative permeability conditions.

It is easier to discuss relative permeability - saturation behavior if effective saturation units are used rather than the pore saturation units used so far. Definitions of these effective saturation units is the subject of the next section.

Effective (Normalized) Saturations

The effective, or normalized, saturation expresses the fluid saturation as a fraction of the mobile fluid(s) range. Effective saturations are usually indicated by a superscript asterisk, such as S_w^* , S_o^* , and S_g^* . In the older literature the symbol S_{oe} was often used. By definition the effective saturations are written in terms of the irreducible wetting phase saturation. Thus for a water-wet reservoir rock condition the effective saturations would be

$$S_w^* = \frac{(S_w - S_{iw})}{(1 - S_{iw})} \quad ; \quad S_o^* = \frac{S_o}{(1 - S_{iw})} \quad ; \quad S_g^* = \frac{S_g}{(1 - S_{iw})} \; .$$

Pore saturations and their corresponding effective saturations for two common reservoir situations are illustrated by the bar displays below.

Irreducible water + Oil + Gas

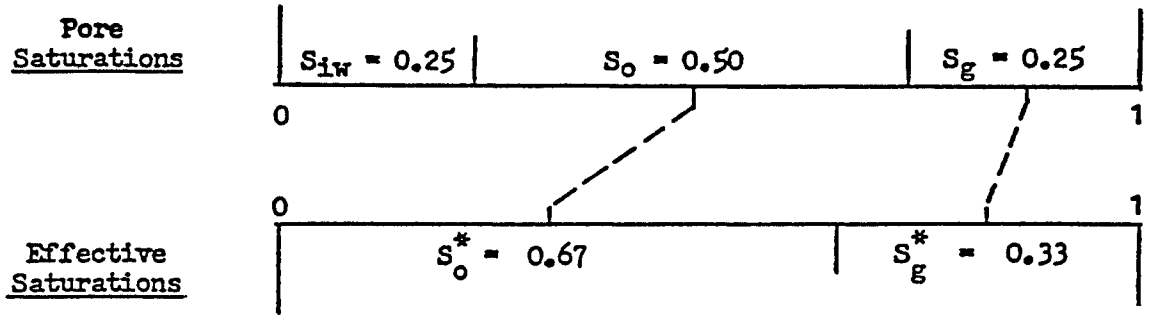

Irreducible water + Mobile water + Oil + Gas

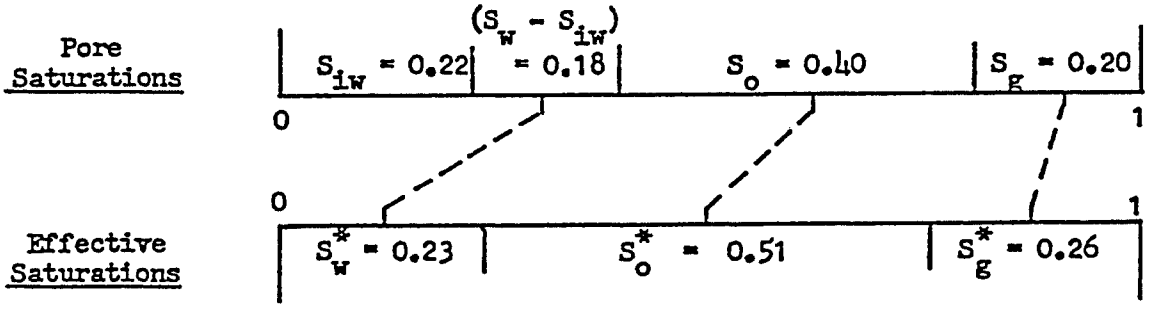

Some reservoir rocks are apparently preferentially oil-wet. In this instance the effective saturations would be written in terms of an irreducible oil saturation as follows:

$$S_o^* = \frac{(S_o - S_{io})}{(1 - S_{io})} \quad ; \quad S_w^* = \frac{S_w}{(1 - S_{io})} \quad ; \quad S_g^* = \frac{S_g}{(1 - S_{io})}$$

Oil would preferentially fill the smallest pores, gas would be located in the largest pores, and water would fill pores of intermediate size.

Theory of Two-Phase Drainage Relative Permeabilities

It was pointed out in the introduction that the effective permeability of a given fluid at a particular saturation condition is a function of pore size distribution of the porous rock, the relative wettability of the fluids to the rock surface, and the saturation history of the rock-fluid system. The same can be said of the relative permeability value.

The object of this section is to develop some general relative permeability relationships in terms of effective saturation units and a definable pore size distribution function. One restriction of these relationships is that they apply only to drainage conditions that is, conditions in which the wetting phase has been or is decreasing. The second restriction is that one of the two fluids wets the rock surface strongly as compared to the second fluid. While these relationships will be completely in terms of "wetting fluid" and "nonwetting fluid," they will be applied later to rock-fluid systems that contain water and oil or water and gas.

To start with, it is well to make the following definitions of terms to be used in this section. Specifically:

S_w = wetting phase saturation, pore volume fraction (not water)

S_n = nonwetting phase saturation, pore volume fraction

S_{iw} = irreducible wetting phase saturation, pore volume fraction

S_w^* = effective wetting phase saturation, $= (S_w - S_{iw})/(1 - S_{iw})$

k_w , k_n = effective permeability, md , of wetting phase and nonwetting phase at a given wetting phase saturation.

$k_w)_{S_w^*=1}$ = effective wetting phase permeability, md , at effective wetting phase saturation equal to 1.

$k_n)_{S_w^*=0}$ = effective nonwetting phase permeability, md , at effective wetting phase saturation equal to 0

k_w^{**} = normalized wetting phase permeability, $= k_w / k_w)_{S_w^*=1}$

k_n^{**} = normalized nonwetting phase permeability $= k_n / k_n)_{S_w^*=0}$

λ = pore size distribution index, defined in Eq.1

Figures 6 and 7 illustrate some of the relationships between the terms defined above. Points A and B in Fig. 6 identify the effective phase permeabilities used to get the normalized permeability values plotted in Fig 7. The normalized permeability could just as well be called a relative permeability

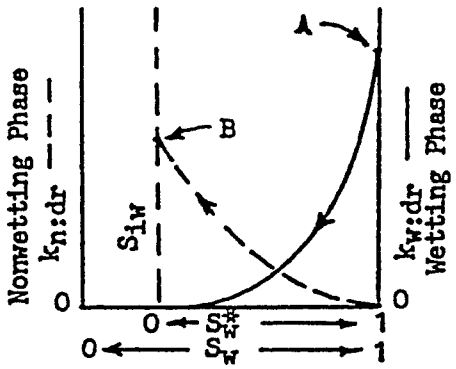

Figure 6

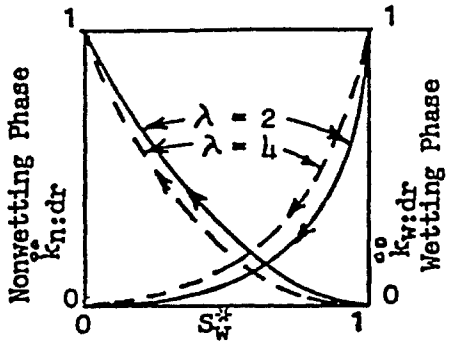

Figure 7

but were not so called in order to reduce confusion later. The two sets of curves in Fig. 7 correspond to different pore size characteristics. The solid curves, $\lambda = 2$, are characteristic of rocks having a wide range of pore sizes, while the dashed curves, $\lambda = 4$, represent a medium range of pore sizes. Curves identified by $\lambda = 2$ are often called "Corey curves" after A.T. Corey, an early researcher of relative permeability behavior. The larger the value of λ, the more uniform the pore size distribution. A lambda value of infinity represents a uniform pore size. Natural sandstones and some limestones are characterized by lambda values between about 0.5 and 4. Lambda between 0.8 and 1.5 represents a good average range of sandstone values.

Lambda is called the pore size distribution index. It can be determined from drainage capillary pressure curves, or from a drainage Leverett J function curve. Brooks and Corey (2,3), on the basis of experimental data, proposed the relationship of Eq. 1 for determining .

$$(P_c/P_e)^{-\lambda} = S_w^* \tag{1}$$

A simpler equation to use is the logarithmic equivalent

$$\log P_c = \log P_e - 1/\lambda \log S_w^* \tag{2}$$

Equation 2 shows that the reciprocal of the slope of a straight line on $\log P_c - \log S_w^*$ coordinates defines λ. Figure 8 shows such plots from air-brine capillary pressure data for two Berea and two Boise sandstone core samples. Effective water saturation values were calculated by reading saturations at which the capillary pressure curves became essentially vertical and designating these values as S_{iw}.

In some instances a plot like Fig. 8 will show slight curvature at low values of S_w^*. Such curvature can be rectified by changing the value of S_{iw}

used in calculating S_w^* . Generally speaking, it is not worth-while considering data at S_w^* values less than about 0.1 when determining λ .

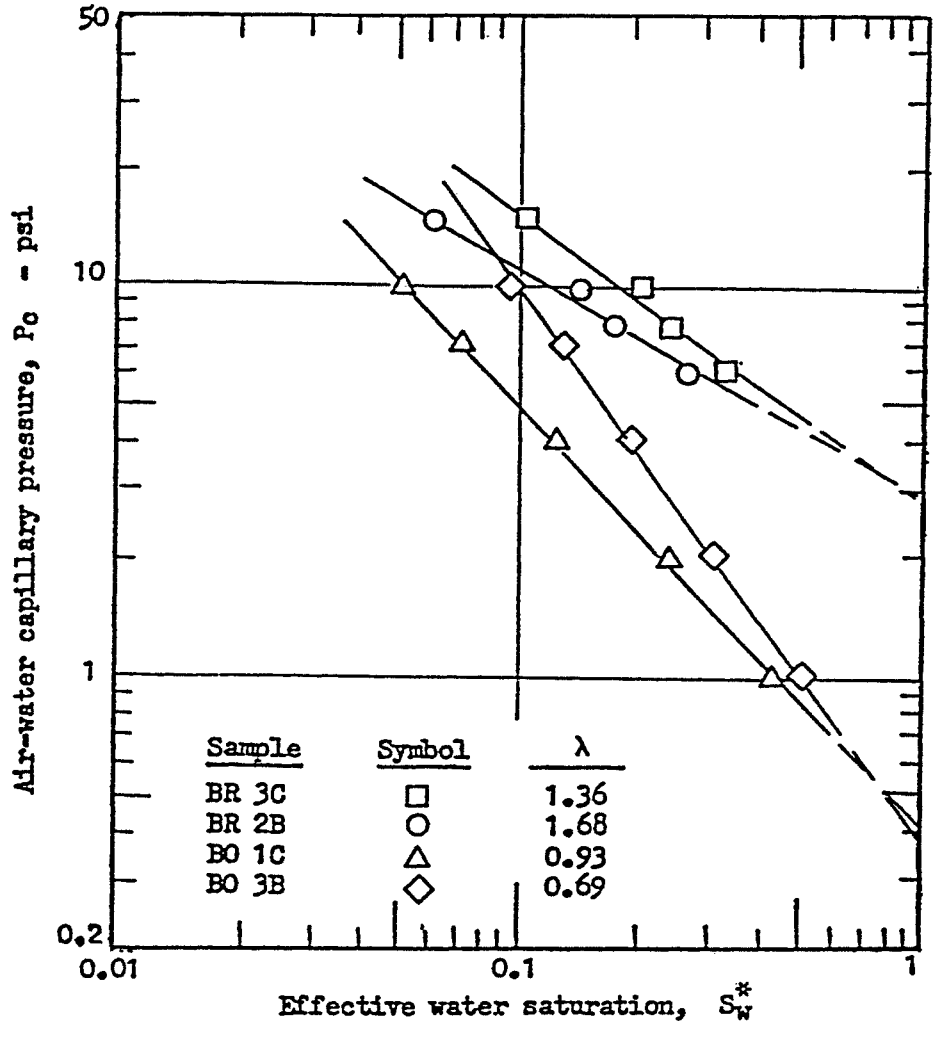

Figure 8. Log-log relationship of capillary pressure and effective water saturation, Boise and Berea sandstone.

It was point out on Page 5 that as effective wetting phase saturation declines from its starting value of unity during the drainage process, changes occur in both the cross-section area of flow and the flow path length of both phases. The early work of Burdine (4) and others associated with Gulf Research and Development Company, led to the following drainage relationships for the two normalized permeabilities:

$$\overset{\circ\circ}{k}_{w:dr} = \frac{k_w}{k_w)_{S_w^*=1}} = (S_w^*)^2 \frac{\int_0^{S_w^*} (1/P_c)^2 \, dS_w^*}{\int_0^1 (1/P_c)^2 \, dS_w^*} \tag{3}$$

for the wetting phase, and

$$\overset{\circ\circ}{k}_{n:dr} = \frac{k_n}{k_n)_{S_w^*=0}} = (1-S_w^*)^2 \frac{\int_{S_w^*}^1 (1/P_c)^2 \, dS_w^*}{\int_0^1 (1/P_c)^2 \, dS_w^*} \tag{4}$$

for the nonwetting phase.

In the above equations, the portions that involve the ratio of integrals of $(1/P_c)^2 \, dS_w^*$ represent flow area changes, while the other terms, $(S_w^*)^2$ and $(1-S_w^*)^2$, represent flow path length changes.

Solutions of Eqs. 3 and 4 can be obtained by several means. When the pore size distribution index, λ, is known, the solutions become:

$$\overset{\circ\circ}{k}_{w:dr} = (S_w^*)^{\frac{2+3\lambda}{\lambda}} \tag{5}$$

for the wetting phase, and

$$\overset{\circ\circ}{k}_{n:dr} = (1-S_w^*)^2 \left[1 - (S_w^*)^{\frac{2+\lambda}{\lambda}} \right] \tag{6}$$

for the nonwetting phase. When the index, λ, is not known, or when the log P_c-log S_w^* plot is not linear in the saturation range of interest, the integral ratios can be evaluated by graphical methods. The following sketches illustrate the graphical method of determining areas under the $(1/P_c)^2$ vs S_w^* curve.

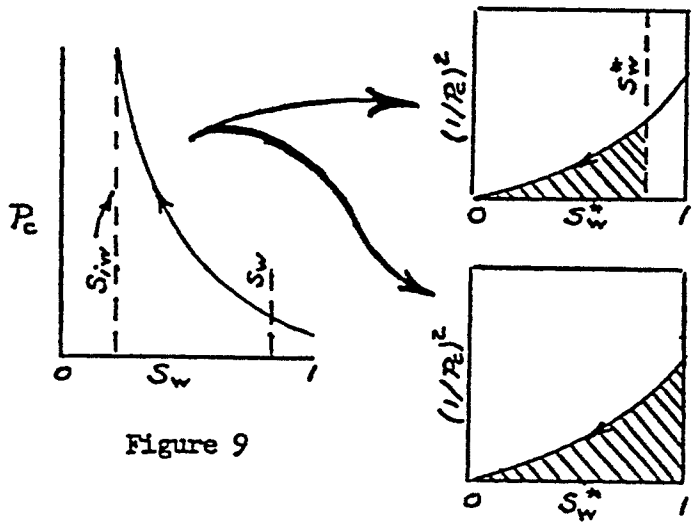

Figure 9

Shaded area under $(1/P_c)^2$ curve equals $\int_0^{S_w^*} (1/P_c)^2 \, dS_w^*$ of Equation 3.

Shaded area under $(1/P_c)^2$ curve equals $\int_0^{1} (1/P_c)^2 \, dS_w^*$ of Equation 3.

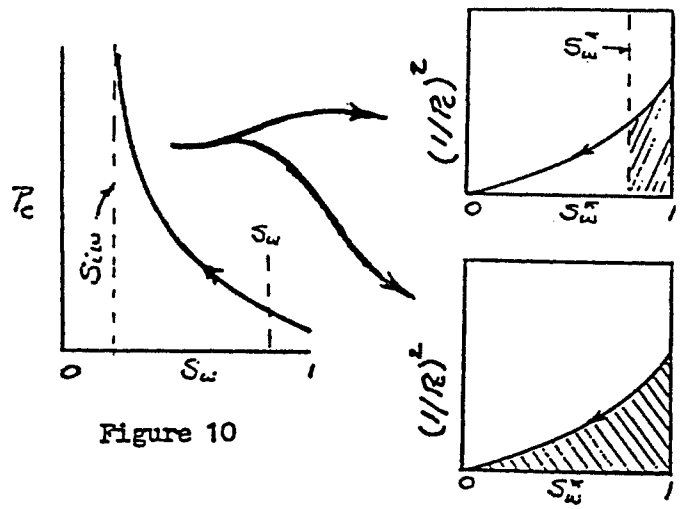

Figure 10

Shaded area under $(1/P_c)^2$ curve equals

$$\int_{S_w^*}^{1} (1/P_c)^2 \, dS_w^*$$

of Equation 4.

Shaded area under $(1/P_c)^2$ curve equals

$$\int_{0}^{1} (1/P_c)^2 \, dS_w^*$$

of Equation 4.

Note that it is not necessary to perform four graphical integrations as indicated by the four sketches above. Two suffice.

Table 1 lists several relationships of normalized permeability and effective wetting phase saturation. The pore size distribution indexes of 2, 4, and ∞ produce the equations proposed by Wyllie (5) to be used for cemented sandstones and oolitic and small-vugular limestones ($\lambda = 2$), poorly sorted unconsolidated sandstones ($\lambda = 4$), and well sorted unconsolidated sandstones ($\lambda = \infty$). The

Table 1

Two-phase Drainage Normalized Permeability Relationships

Porous Media Characteristics	λ	$k_{w:dr}^{**}$ (Eq. 5)	$k_{n:dr}^{**}$ (Eq. 6)
Very wide range of pore size	0.5	$(S_w^*)^7$	$(1-S_w^*)^2 (1 - (S_w^*)^5)$
Wide range of pore size	2	$(S_w^*)^4$	$(1-S_w^*)^2 (1 - (S_w^*)^2)$
Medium range of pore size	4	$(S_w^*)^{3.5}$	$(1-S_w^*)^2 (1 - (S_w^*)^{1.5})$
Uniform pore size	∞	$(S_w^*)^3$	$(1 - S_w^*)^3$

pore size distribution index of 2 yields the so-called Corey equations that are used extensively in reservoir engineering calculations when nothing specific is known of the porous media characteristics. My experience, however, is that a pore size index in the range of 0.6 to 1 is more frequently encountered than an index of 2.

The next two sections will show how the normalized permeability relationships given by Eqs. 5 and 6 and Table 1 can be adjusted to relative permeabilities based on absolute permeability. The first section considers adjustments that will compensate for the amount of irreducible wetting phase present. The second section concerns an adjustment of the nonwetting phase relationship to accommodate critical saturation and/or stratification effects.

Adjusting Normalized Permeabilities for S_{iw}. The relationship of normalized permeability and effective wetting phase saturation given by Eq. 5 can be used directly to represent relative permeability of the wetting phase as a function of effective saturation. This is because the base of the normalized permeability is $k_w)_{S_w^*=1}$, which is also the absolute permeability of the porous media, k. Consequently, the following relationships apply :

$$\underbrace{k_w^{\bullet\bullet} = \frac{k_w}{k_w)_{S_w^*=1}}}_{\text{definition}} = \underbrace{\frac{k_w}{k}}_{\text{definition}} = k_{rw} \tag{7}$$

Therefore,

$$k_{rw:dr} = \left(S_w^* \right)^{\frac{2+3\lambda}{\lambda}} \tag{8}$$

On the other hand, it is always necessary to discount the normalized nonwetting phase permeability to obtain a corresponding relative permeability. This is because the base of the nonwetting phase normalized permeability is $k_n)_{S_w^*=0}$, which is always less than the absolute permeability of the porous media. The necessary discount factor is the effective nonwetting phase permeability at irreducible wetting phase saturation, $k_n)_{S_{iw}}$. This can be shown as follows :

$$\underbrace{k_n^{\bullet\bullet} = \frac{k_n}{k_n)_{S_w^*=0}}}_{\text{definition}} = \frac{k_n}{k_n)_{Siw}} \tag{9}$$

Multiplying both sides of this equation by $\frac{k_n)_{Siw}}{k}$ yields

$$k_n^{\bullet\bullet} \cdot \frac{k_n)_{Siw}}{k} = \frac{k_n}{k_n)_{Siw}} \cdot \frac{k_n)_{Siw}}{k} = \frac{k_n}{k} \tag{10}$$

Letting the relative permeability term $\frac{k_n)_{S_{iw}}}{k}$ be symbolized by k_r^o, Eq. 10 becomes

$$k_n\, k_r^o = \frac{k_n}{k} = k_{rn} \tag{11}$$

Substituting the relationship of Eq. 6 for k_n yields the following nonwetting phase relative permeability equation:

$$k_{rn:dr} = k_r^o\,(1-S_w^*)^2\left[1 - (S_w^*)^{\frac{2+\lambda}{\lambda}}\right] \tag{12}$$

In order to make effective use of Eq. 12, it is necessary to relate k_r^o to the irreducible wetting phase saturation, S_{iw}. It is to be expected that the larger the irreducible wetting phase, the smaller will be the value of k_r^o. This follows because the irreducible wetting phase acts to reduce the cross-section of area of flow of the nonwetting phase and increase its flow path length. It is also expected that any relationship of k_r^o and S_{iw} should show some effect of pore size distribution.

To my knowledge, no one has shown how λ affects k_r^o at various values of S_{iw}. Neither has a correlation of k_r^o and S_{iw} been published. Considerable laboratory test data are available, however, to develop correlations for specific rocks. Commercial laboratories normally list air permeability and the nonwetting phase effective permeability at residual wetting phase saturation in their laboratory results. A value for k_r^o can be obtained by correcting the air permeability to absolute permeability and dividing it into the measured $k_n)_{S_{iw}}$ value.

Figure 11 shows the result of plotting k_r^o, calculated as above, against S_{iw} for approximately 35 sandstone core samples. S_{iw} values fell between 0.2 and 0.5. While the data showed considerable scatter, the trend line is useful when direct information is unavailable. The curve of Fig. 11 has the relationship

$$k_r^o = 1.31 - 2.62\, S_{iw} + 1.1\, (S_{iw})^2 \tag{13}$$

This relationship should not be used at $S_{iw} > 0.5$. At S_{iw} values less than 0.12, the value of k_r^o should be taken as unity.

Equations 8, 12, and 13 are useful general relationships for calculating two-phase drainage relative permeability values. Differentiating the equations with respect to S_w and evaluating the derivatives at the end-point saturations yields the following information:

$$\left.\frac{dk_{rw}}{dS_w}\right|_{S_w=1} = \left(\frac{2+3\lambda}{\lambda}\right)\left(\frac{1}{1-S_{iw}}\right) \tag{14}$$

$$\left.\frac{dk_{rw}}{dS_w}\right|_{S_{iw}} = 0 \tag{15}$$

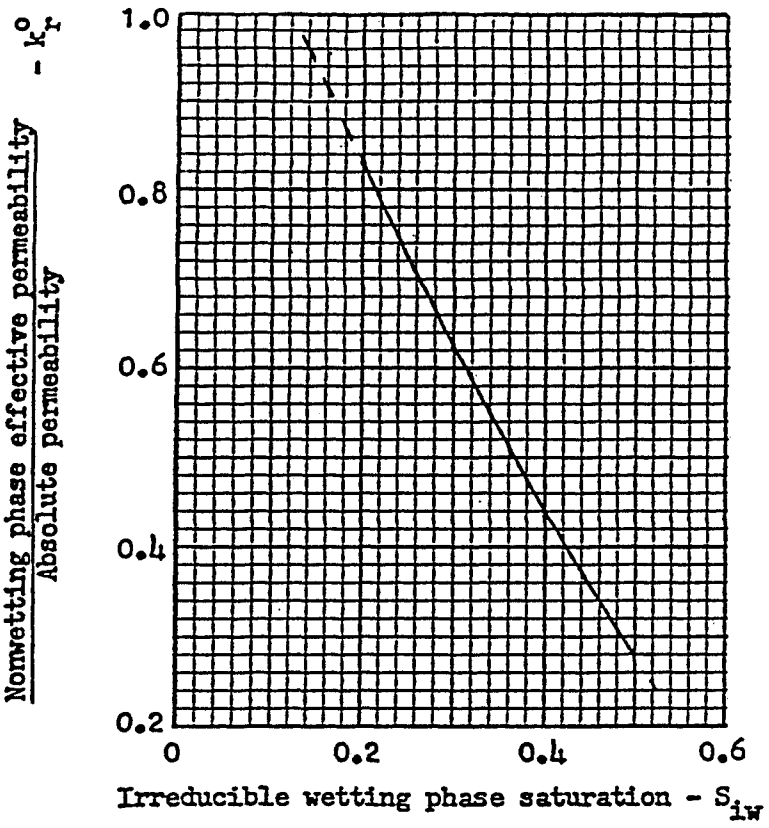

Figure 11. Average curve of nonwetting phase relative permeability at irreducible wetting phase saturation

Thus, the wetting phase curve leaves $k_{rw:dr} = 1$ with a slope indicated by Eq. 14, and terminates at $k_{rw:dr} = 0$ with zero slope. Equations 16 and 17 show that the nonwetting phase curves starts with zero slope at $k_{rn:dr} = 0$, and terminates at the irreducible saturation with a value of k_r^o and a slope of $(-2\ k_r^o/(1-S_{iw}))$.

$$\left.\frac{dk_{rn}}{dS_w}\right|_{S_w=1} = 0 \qquad (16) \qquad\qquad \left.\frac{dk_{rn}}{dS_w}\right|_{S_{iw}} = \frac{-2k_r^o}{(1-S_{iw})} \qquad (17)$$

Adjusting k_{rn} for Critical Saturation and/or Stratification Effects. As indicated by Eq. 16, the slope of the nonwetting phase relative permeability curve as it leaves its origin ($S_w = 1$; $k_{rn} = 0$) is zero. As nonwetting phase saturation develops the relative permeability curve increases continuously in slope and magnitude. This is illustrated by Curve A, Fig. 12, which is a graphic representation of Eqs. 12 and 13 for conditions of $\lambda = 2$; $S_{iw} = 0.2$.

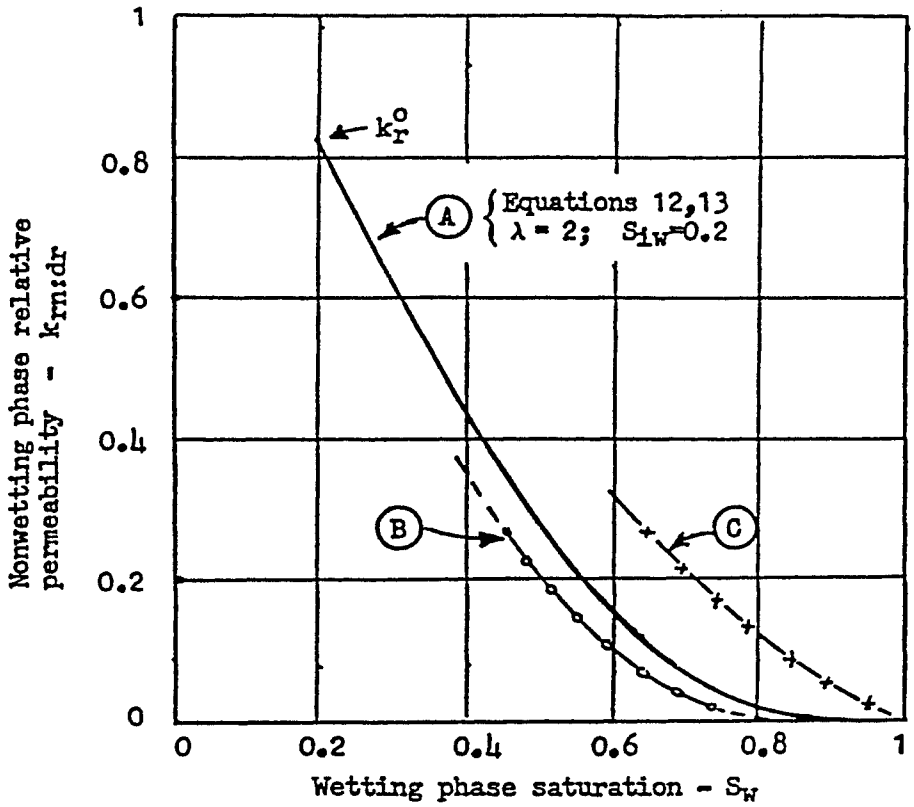

Figure 12. Graph illustrating the effect of critical saturation and/or stratification on nonwetting phase drainage relative permeability curves.

When results of laboratory tests on core plugs are plotted on the coordinates of Fig. 12, the nonwetting phase relative permeability curves often show trends that differ from those of Curve A. Curve B, for example, while exhibiting the same general shape as A, apparently starts from a saturation value (determined by extrapolation) somewhat less than unity. Curve C, on the other hand, starts from the $S_w = 1$; $k_{rn:dr} = 0$ coordinate with a very definite slope and is straighter.

One explanation of the behavior of Curve B involves the so-called "critical saturation" effect. The idea here is that while the nonwetting phase saturation is less than some critical value, the nonwetting phase is distributed throughout the pore system as unconnected islands of saturation, and can not flow. At saturations greater than critical, the islands have become connected so that a continuous path exists to conduct nonwetting phase. One often hears the term "critical saturation" in relation to gas saturation; i.e., "critical gas saturation". However, the critical saturation effect explained above is a property of the nonwetting phase and is just as applicable to oil in an oil-water system as it

is to gas in a gas-water or gas-oil-water system.

While the above description seems to explain the relationship of the A and B curves of Fig. 12, it fails to explain the behavior of Curve C. Corey and Rathjens (6) have shown that stratification within the core can affect laboratory results. They found that measurements made on the same core gave different relative permeability curves when flow was parallel to bedding and when flow was perpendicular to bedding. Parallel-to-bedding flow tended to yield $k_{rn:dr}$ values that increased very rapidly, as illustrated by Curve C. Perpendicular-to-bedding flow tended to yield curves more akin to Curves A and B. It appears then, that stratification effects have some influence on the shape and position of relative permeability curves.

Whether the above described nonwetting phase relative permeability behavior results from critical saturation effects or from stratification effects is not clear. Obviously, though, Eq. 12 is of limited usefulness because it can not duplicate observed behavior of many rock-fluid systems. Better agreement of calculated and measured relative permeability curves can be obtained when Eq. 12 is modified in the manner proposed by Corey (7). This is to incorporate an additional wetting phase saturation parameter, S_m, into Eq. 12 so that the term $(1 - S_w^*)^2$ becomes $(1 - (S_w - S_{iw})/(S_m - S_{iw})^2$. Equation 12 then becomes

$$k_{rn:dr} = k_r^o \left[\frac{S_m - S_w}{S_m - S_{iw}}\right]^2 \left[1 - (S_w^*)^{\frac{2+\lambda}{\lambda}}\right] \qquad (18)$$

The wetting phase saturation parameter, S_m, has no physical significance. It is simply a variable in Eq. 18 that partially controls the shape and position of the nonwetting phase drainage corve. Figure 13 shows $k_{rn:dr}$ curves calculated from Eq. 18 for various S_m values. Other parameters are $\lambda = 2$ and $S_{iw} = 0.2$.

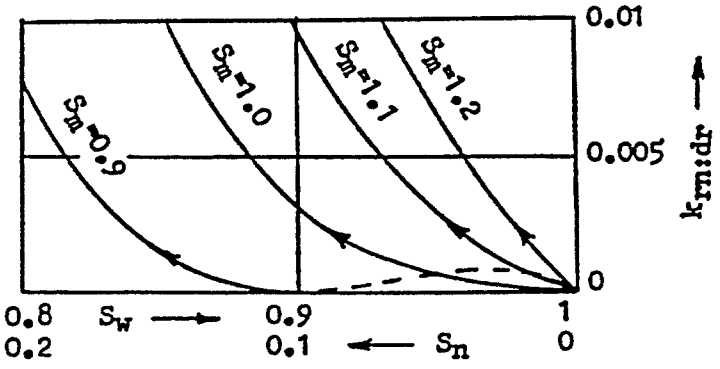

Figure 13

As illustrated by the S_m=0.9 curve, behavior suggestive of critical saturation effects are obtained when S_m is less than 1: that is, the curve is zero valued and has zero slope at $S_w = S_m$. Note also that Eq. 18 will yield invalid $k_{rn:dr}$ values (dashed line) when $S_m < S_w < 1$. The $S_m = 1$ curve also has zero value and

zero slope where $S_w = S_m$. At S_m values greater than 1 the characteristic of having zero slope at the saturation of origin no longer holds. All curves originate at the $k_{rn;dr}=0$; $S_w=1$ coordinate, have increasing slope values at the origin, and are straighter. This is clearly shown by the $S_m=1.1$ and $S_m=1.2$ curves.

Because of the added variable, S_m , Eq. 18 has much greater applicability to reservoir engineering calculations than Eq. 12. Comparison of a number of laboratory measured $k_{rn:dr}$ values with those calculated from Eq. 18 indicate that S_m usually falls between 0.9 and 1.1 and is seldom greater than 1.3.

The next section presents two simplified reservoir engineering calculations that illustrate use of the relative permeability relationships developed so far.

Example Use of Two-Phase Drainage Relationships. It is, perhaps, worthwhile to restate conditions to which Eqs. 8 and 18 apply in reservoir calculations before going into the illustrative calculations. These are:

1. Two phases. In petroleum reservoirs, these would normally be gas-water or oil-water systems. Thus the relationships could be used in calculations that pertain to gas cap or oil zone conditions.
2. Drainage. Wetting phase saturation change previous to or during the time of calculation must be in a decreasing direction. It is generally believed that hydrocarbons migrate into and displace original water from petroleum-bearing structures. Thus, drainage conditions would apply to calculations concerned with initial conditions in the reservoir.
3. Wettability. One of the two phases must wet the rock matrix strongly in preference to the other phase. Under cas cap conditions water is always the wetting phase. Under oil zone conditions water is usually the wetting phase.

Water is considered the wetting phase and either gas or oil the nonwetting phase in the example calculations that follow. The symbol $k_{rw:dr}$ will therefore identify water relative permeability values. Likewise, symbols $k_{rg:dr}$ and $k_{ro:dr}$ will identify gas and oil relative permeability values.

Example A illustrates the calculation of a probable producing water-oil ratio if the well is completed in a given section. The section lies within the so-called transition zone, so the water has some degree of mobility. Should the calculated water-oil ratio be greater than 1, say, it might not be profitable to complete the well in this section.

Example A. Calculation of Probable Water-oil Ratio

Given: Average conditions in the completion interval are believed to be as follows:

	Oil	Water	Source of data
Fluid saturations, S	0.45	0.55	E log calculations
Irreducible water saturation, S_{iw}		0.30	Guestimate
Fluid viscosity, μ cp	3	0.5	Est. from °API, °F
Formation vol. factors, B	1.2	1.05	Est. from °API, °F
Pore size distribution index, λ	2		Assumed
Stratification factor, S_m	1		Assumed

Solution: Water-oil ratio is calculated from radial flow equations for each phase separately. After canceling common parameters, the ratio is:

$$q_w/q_o = \frac{k_w \cdot \mu_o B_o}{k_o \mu_w B_w} = \frac{k_{rw:dr} \mu_o B_o}{k_{ro:dr} \mu_w B_w}$$

$$S_w^* = (S_w - S_{iw})/(1 - S_{iw}) = (0.55-0.30)/(1-0.30) = 0.357$$

$$k_{rw:dr} = (S_w^*)^{\frac{2+3\lambda}{\lambda}} = (0.357)^4 = 0.0163$$

$$k_{ro:dr} = k_r^o \left((S_m - S_w)/(S_m - S_{iw})\right)^2 \left(1 - (S_w^*)^{\frac{2+\lambda}{\lambda}}\right)$$

$$k_r^o = 1.31 - 2.62\, S_{iw} + 1.1\, S_{iw}^2 = 0.623$$

$$k_{ro:dr} = 0.623 \left((1-0.55)/(1-0.30)\right)^2 \left(1 - (0.357)^2\right) = 0.225$$

Therefore

$$q_w/q_o = (0.0163 \cdot 3 \cdot 1.2)/(0.225 \cdot 0.5 \cdot 1.05) = 0.5$$

Comments: Note the low value of the water relative permeability, 0.016 , even though water fills 55 percent of the pore space. This illustrates the asymtotic-to-zero shape of the water curve when approaching the irreducible saturation value.

Example B illustrates the calculation of gas relative permeability values in a limited range of gas saturation. In this example the pore size distribution index and the irreducible water saturation values are obtained from a laboratory capillary pressure curve.

Examole B. Calculation of Gas Relative Permeability Values

Given : A study is being made of storing gas by injecting it into an aquifer. Calculations require values of gas relative permeability in the gas saturation range between zero and 20%. Laboratory determined capillary pressure-saturation data for air displasing 5000 ppm brine are available on a typical core sample from the zone of interest. It is assumed that critical gas saturation will be 5%.

Capillary Pressure Data

P_c psi	Brine Saturation fraction
0.5	0.965
1.0	0.713
2.0	0.483
4.0	0.347
8.0	0.266
16.0	0.219
32.0	0.191
300	0.160

Solution : Values of S_w^* calculated from the capillary pressure data using the 300 psi saturation value of 0.16 as the irreducible water saturation value are plotted against capillary pressure as shown. From the plot the slope of the straight line is - 1.24. Llambda is, therefore, 0.81. Other parameters are as follows:

$$\frac{2+\lambda}{\lambda} = 3.47$$

$S_{iw} = 0.16$

$k_r^o = 0.92$

$S_m = 0.95$

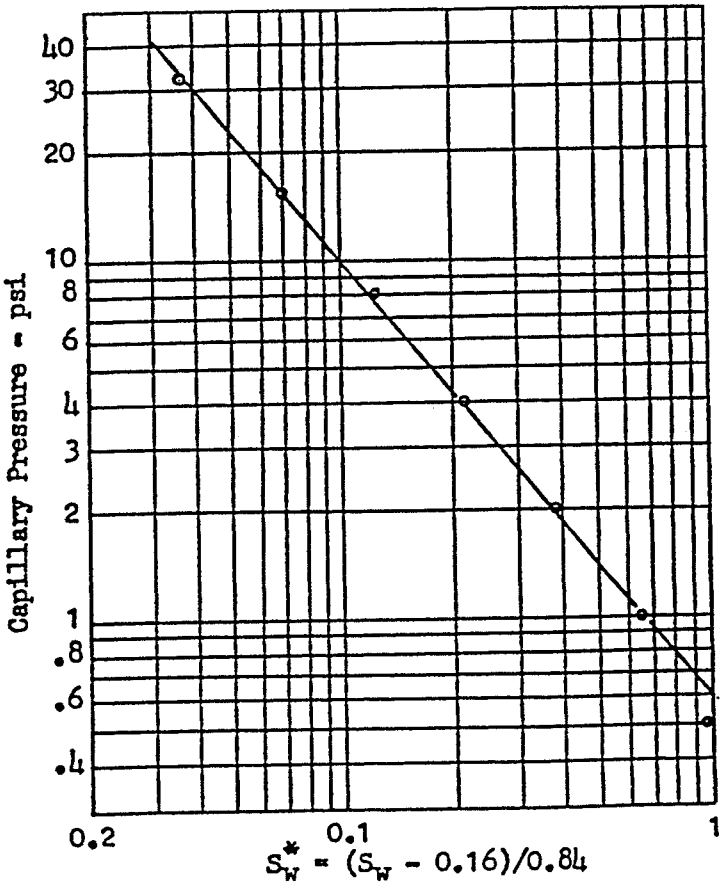

Gas relative permeability values are calculated by use of Eq. 18 as shown on the following page.

$$k_{rg:dr} = k_r^o \left[\frac{S_m - S_w}{S_m - S_{iw}}\right]^2 \left[1 - (S_w^*)^{\frac{2+\lambda}{\lambda}}\right]$$

S_g	S_w	S_w^*	$\left[\frac{S_m - S_w}{S_m - S_{iw}}\right]^2$	$(S_w^*)^{3.47}$	$\left[1 - (S_w^*)^{3.47}\right]$	$k_{rg:dr}$
0.00	1.00	1.000	0.00400	1.000	0.000	0.000000
0.05	0.95	0.940	0.00000	0.808	0.192	0.000000
0.08	0.92	0.905	0.00144	0.707	0.293	0.000387
0.11	0.89	0.869	0.00577	0.614	0.368	0.00205
0.14	0.86	0.833	0.0130	0.531	0.469	0.00560
0.17	0.83	0.798	0.0231	0.456	0.544	0.0115
0.20	0.80	0.762	0.0361	0.389	0.611	0.0203

Comments : Note that in drawing the straight line on the P_c vs S_w^* plot, the entry pressure point was given little weight. Entry pressure points often do not correlate well with the other points. The capillary pressure data were for a single core - hopefully it is typical of the formation as a whole. If capillary pressure data are available on a number of core samples it is generally better to normalize the capillary pressure data into the form of the Leverett J function and use the J-function to determine λ and S_{iw}. The assumed critical gas saturation of 5% was, of course, an independent choice. Had a different value been selected, the gas relative permeability values would have been considerably different.

Probably, the majority of reservoir engineering calculations involve conditions in which three phases, gas, oil, and water, are present in pore structure. The general concepts and theories used previously to develop two-phase drainage relative permeability relationships are extended in the next section to three-phase drainage relationships.

Three-phase Drainage Relative Permeability Relationships.

It will be recalled from previous theory that the relative permeability value that a particular phase exhibits depends, in part, on the radii or size of the pores that contain the phase. Also, that under drainage conditions (nonwetting phase displacing wetting phase) the nonwetting phase tends to be located in the larger pores while the wetting phase tends to be in smaller pores. The resulting distribution of phases, at a particular saturation condition, was illustrated in Fig. 4 , page 4.

In dealing with three phases it is necessary to consider in greater detail the relative affinity of the phases for the rock surfaces and the sequence of phase displacements that led to the saturation state of interest. These factors have a bearing on the pore sizes in which the three fluids will be located and consequently an effect on their relative permeability values at the particular saturation. In this section of the notes water will be considered to have the strongest affinity for the rock surfaces (most wetting phase), oil will be considered to have an intermediate wettability, and gas to be the least wetting phase. The displacement sequence will be that water initially occupied all pore space but a portion was displaced by oil. Later, a portion of the oil was displaced by gas.* As a consequence of this preferential wettability situation and the two displacements the resulting distribution of the three phases in the pore structure is visualized as sketched in Fig. 14 . Irreducible water remains in pores of size range (a → b). Mobile water that was not displaced by oil occupies pores of size range (b → c). Oil and gas phases occupy pores of size range (c → d) and (d → e). The question now becomes how to use this

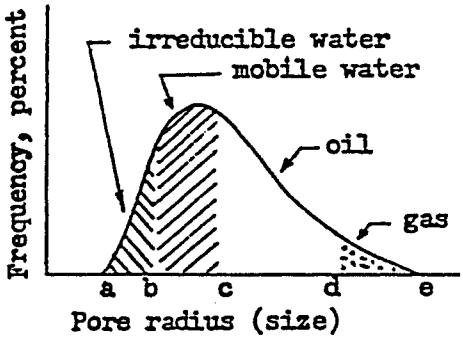

Figure 14

* Note that this two-step displacement process of oil displacing water and in turn being partially displaced by gas is generally in line with the displacement processes in oil fields that produce by solution gas drive or by expanding gas cap drive. It is generally thought that during the formative stages of an oil field that oil migrates into a trap and displaces part of the water there initially. Gas displaces oil during the production phase of operations.

idealized fluid distribution model to develop useful three-phase relative permeability equations.

Corey, Rathjens, Henderson, and Wyllie (8) were perhaps the first to publish a set of three-phase relative permeability equations. Their equations were based on results of laboratory relative permeability measurements on cores from several sources. Basically their experiments consisted of comparing gas and oil relative permeability - saturation curves obtained under different drainage test procedures. In the first set of tests the core was saturated 100 % with $CaCl_2$ brine. Brine was then displaced by oil under controlled capillary pressure conditions to some lower saturation. The core was then desaturated further by displacing a portion of the oil by gas. The second displacement was also under controlled capillary pressure conditions. The resulting fluid distribution in the pore structure is illustrated by Fig. 14 .

The second set of tests used the same core but eliminated the use of the $CaCl_2$ brine. Gas displaced oil - always under two-phase conditions. Refering to Fig. 14 , pore size range (a → b) would contain irreducible oil and mobile oil would fill pore size range (b → d).

The important result of these tests came from comparing the gas relative permeability - gas saturation curves of the two tests. They were found to be the same, within experimental error. Corey et al hypothesized that this behavior indicated that oil displacement by gas was 100 % effective in pores which previously had experienced water displacement by oil. To put it differently, when oil displaced water in pore size range (d → e) of Fig. 14 there could be some residual water remaining because of entrappment in individual pores and/or adsorption on rock surfaces. When gas displaced oil from this same range of pores sizes, there was no additional entrappment or adsorption of liquid (oil). Carrying this hypothesis to its extreme means that water will constitute the only residual liquid (or irreducible liquid) remaining from an oil - water displacement process that is followed by a gas - oil displacement. Whether this hypothesis is valid for all, or most, pore structures is questionable (the Corey tests were on only a limited number of cores having pore size distribution indexes near 2), but it remains a very basic factor in the three-phase relative permeability equations that will be developed further along.

One important implication of the Corey et al hypothesis is that the same basic methods apply to the calculation of two-phase and three-phase drainage curves. Refering back to Eqs. 3 and 4 on page 11 it will be seen that for the

two-phase systems the normalized permeability values were products of the square of their effective saturations and a ratio of integrated values of the $1/P_c$ vs S_w^* relationship. (Note that the subscript w here refers to wetting phase and not water). Under the "no residual oil" hypothesis three-phase relationships can be developed by changing the variable of integration from effective wetting phase saturation, S_w^*, to effective total liquid saturation, S_L^*. This results in the following three equations for normalized permeabilities :

for the mobile water phase,

$$k_w]_{dr} = \frac{k_w}{k_w)_{S_w^*=1}} = (S_w^*)^2 \frac{\int_0^{S_w^*} \frac{dS_L^*}{P_c^2}}{\int_0^1 \frac{dS_L^*}{P_c^2}} \quad ; \qquad (19)$$

for the oil phase,

$$k_o]_{dr} = \frac{k_o}{k_o)_{S_o^*=1}} = (S_o^*)^2 \frac{\int_{S_w^*}^{S_L^*} \frac{dS_L^*}{P_c^2}}{\int_0^1 \frac{dS_L^*}{P_c^2}} \quad ; \qquad (20)$$

and for the gas phase,

$$k_g]_{dr} = \frac{k_g}{k_g)_{S_g^*=1}} = (S_g^*)^2 \frac{\int_{S_L^*}^1 \frac{dS_L^*}{P_c^2}}{\int_0^1 \frac{dS_L^*}{P_c^2}} \qquad (21)$$

where

$$S_w^* = \frac{S_w - S_{iw}}{1 - S_{iw}} \quad ; \quad S_o^* = \frac{S_o}{1 - S_{iw}} \quad ; \quad S_g^* = \frac{S_g}{1 - S_{iw}} \qquad (22)$$

and

$$S_L^* = S_w^* + S_o^* = \frac{S_w + S_o - S_{iw}}{1 - S_{iw}} = 1 - S_g^* \qquad (23)$$

Again, as in the case of the comparable two-phase relationships (Eqs 3 and 4) there are two ways of solving Eqs 19 - 21. When capillary pressure - effective water saturation values form a straight line on log-log coordinates (as illustrated by Fig. 8) analytical solutions can be obtained in terms of the pore size distribution index, λ, and the irreducible water saturation S_{iw}. These

solutions may be of several forms, but the following three are perhaps the most useful. Note that these are relative permeabilities on an absolute permeability base. As can be seen both the gas and oil equations incorporate k_r^o to adjust for the irreducible water saturation. The gas phase equation incorporates S_m to permit adjusting for critical gas saturation effects.

For the mobile water phase,

$$k_{rw}\Big]_{dr} = \frac{k_w}{k} = \left(\frac{S_w - S_{iw}}{1 - S_{iw}}\right)^{\frac{2+3\lambda}{\lambda}} = (S_w^*)^{\frac{2+3\lambda}{\lambda}} \qquad (24)$$

For the oil phase,

$$k_{ro}\Big]_{dr} = \frac{k_o}{k} = k_r^o \cdot \left(\frac{S_o}{1 - S_{iw}}\right)^2 \left[\left(\frac{S_o + S_w - S_{iw}}{1 - S_{iw}}\right)^{\frac{2+\lambda}{\lambda}} - \left(\frac{S_w - S_{iw}}{1 - S_{iw}}\right)^{\frac{2+\lambda}{\lambda}}\right] \qquad (25)$$

$$= k_r^o \cdot (S_o^*)^2 \cdot \left[(S_L^*)^{\frac{2+\lambda}{\lambda}} - (S_w^*)^{\frac{2+\lambda}{\lambda}}\right] \qquad (26)$$

For the gas phase,

$$k_{rg}\Big]_{dr} = \frac{k_g}{k} = k_r^o \cdot \left(\frac{S_g + S_m - 1}{S_m - S_{iw}}\right)^2 \cdot \left[1 - \left(\frac{S_o + S_w - S_{iw}}{1 - S_{iw}}\right)^{\frac{2+\lambda}{\lambda}}\right] \qquad (27)$$

$$= k_r^o \cdot \left(\frac{S_g + S_m - 1}{S_m - S_{iw}}\right)^2 \cdot \left[1 - (1 - S_g^*)^{\frac{2+\lambda}{\lambda}}\right] \qquad (28)$$

When the log P_c - log S_L^* curve is not linear within the saturation range probably the next best approach is to prepare a plot of $1/P_c^2$ vs S_L^* and to determine areas under the curve that will correspond to various fluid saturation conditions. The areas may be determined graphically (such as counting squares) or the curve can be fit by a simple equation and the integration performed on the equation. The areas so determined represent the numerator of the integral ratios in Eqs. 19 - 21. The denominator is, of course, the sum of the three individual fluid areas. In accordance with Eqs. 19 - 21 the ratio of areas are multiplied by the square of the appropriate effective liquid saturation. The procedure of determining areas graphically is illustrated in Fig. 15 .

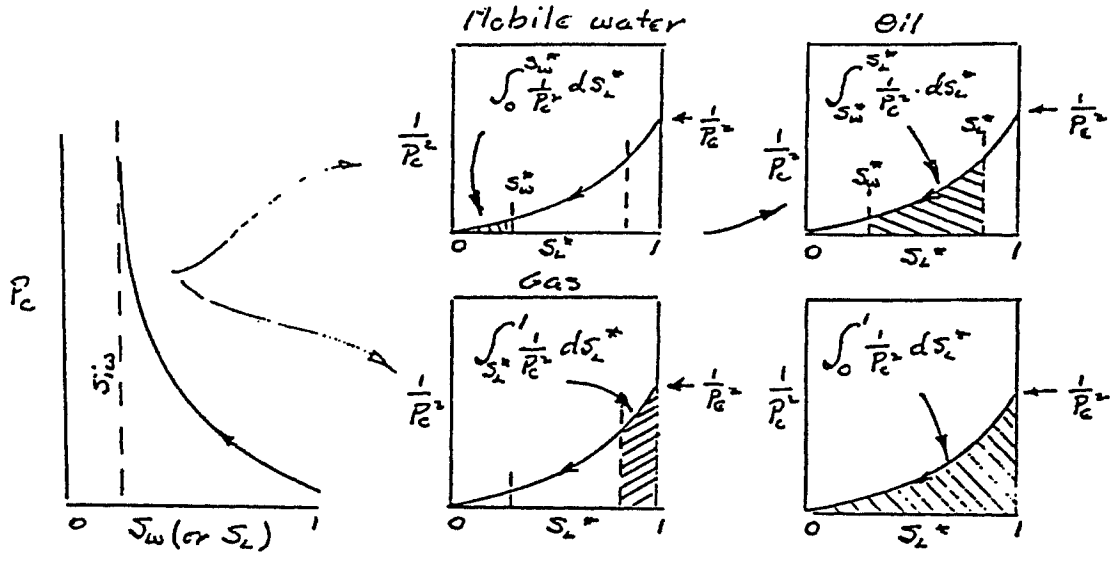

Figure 15

Having developed a set of equations for relative permeability of water, oil, and gas as functions of saturation and rock character it is of interest to see what the resulting curves might look like. Probably the majority of reservoir calculations are for conditions in which the water saturation is at, or close to, the irreducible value. At this condition the water relative permeability is zero and the oil and gas equations take on the form of Eqs. 8 and 12 with oil being the wetting phase. Figs. 16a and 16b show the shapes of typical k_{ro} and k_{rg} curves for S_{iw} values of 0.2 and 0.4 . Note that because of the "no residual oil" hypothesis discussed previously the k_{ro} curve terminates at the S_{iw} value. Also note that k_{ro} remains essentially zero valued over almost one-third of the effective oil saturation range. By refering to Fig. 7 it can be seen that for a rock having a pore size distribution index of unity, $\lambda = 1$, the oil curve would be lower and the gas curve higher.

Fig. 16c shows the shape of the oil and gas curves with 20 % irreducible water and 20 % mobile water present. Although the mobile water fills one-fifth of the pore volume its relative permeability calculates to be only 0.0039 because of its location in the smaller pores. The oil and gas curves appear to be much the same as those of Fig. 16b , however there are small differences in the values of k_{ro} and k_{rg} at a given value of S_g .

Fig. 17 illustrates how several variables affect gas-oil relative permeability ratio curves. Fig. 17a shows the usual behavior of k_{rg}/k_{ro} becoming larger as

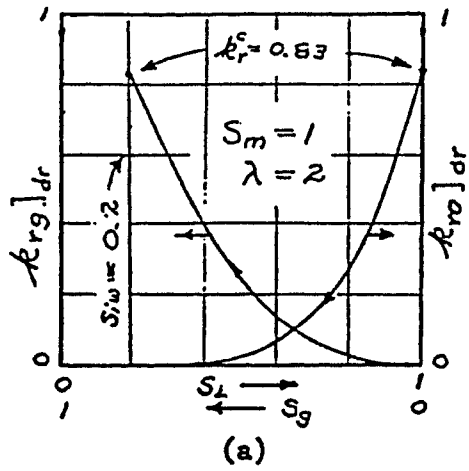

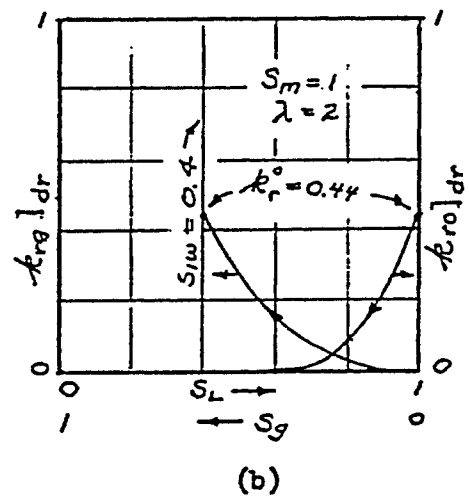

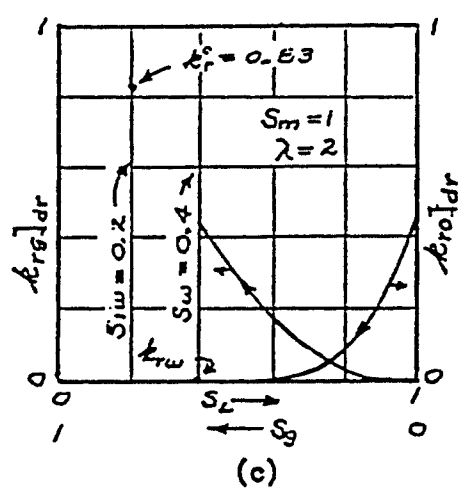

Figure 16

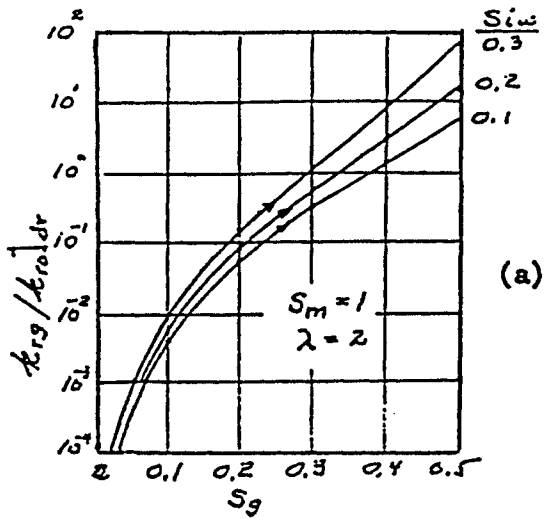

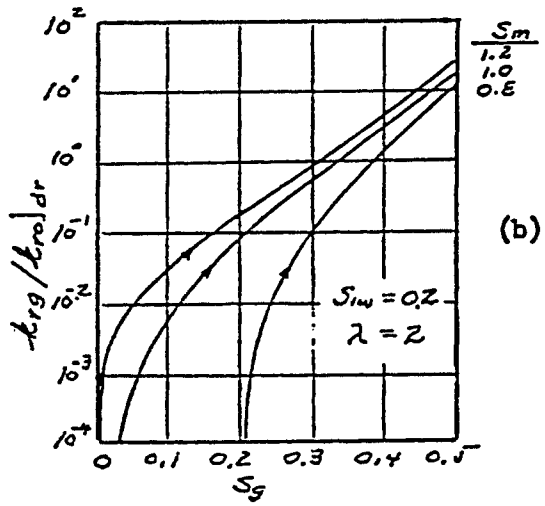

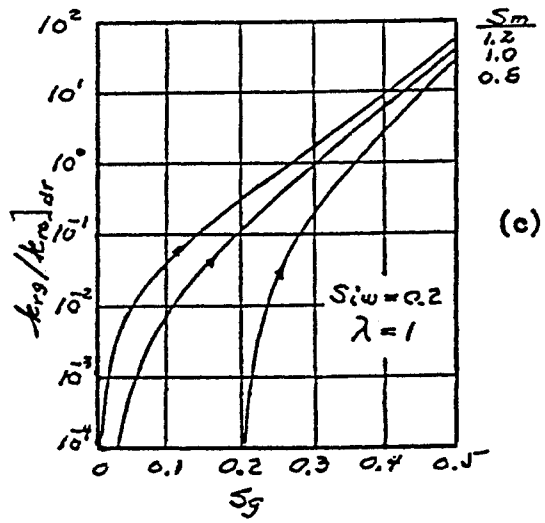

Figure 17

S_{iw} increases. Had the plots been continued to higher values of gas saturation the curves would approach being vertical as S_g approaches $(1 - S_{iw})$. Figs. 17b and 17c show the effect of critical gas saturation on the gas-oil relative permeability ratio curves. Note that S_m has a very nonlinear effect on the ratio curves in the low gas saturation region. The effect of lowering λ from 2 to 1 is to raise the ratio curve and make it slightly more vertical.

Before illustrating the development of relative permeability data for use in reservoir engineering calculations it is pertinent to note other three-phase relationships that appear in the literature. Wyllie (5) presents the following table in Frik's Petroleum Production Handbook. The relations in the table are slight variations of equations published by Corey and Rathjens(6) and Wyllie and Gardner (9).

Table 2. Wyllie's Equations for Three-phase Relative Permeabilities.

Type of formation	k_{rw}	k_{ro}	k_{rg}
Unconsolidated sand, well sorted grains.	$(S_w^*)^3$	$\frac{S_o^3}{(1 - S_{iw})^3}$	$\frac{S_g^3}{(1 - S_{iw})^3}$
Cemented sandstones, oölitic limestones, vugular rocks.	$(S_w^*)^4$	$\frac{S_o^2 (2S_w + S_o - 2S_{iw})}{(1 - S_{iw})^4}$	$\frac{S_g^2 [(1-S_{iw})^2 - (S_L-S_{iw})^2]}{(1 - S_{iw})^4}$

The above equations have a number of restrictions. In the first place all apply to zero critical gas saturation - that is, for the condition of $S_m = 1$. Secondly, the hydrocarbon equations do not take into account k_r^o. In early publications originating from Gulf Research and Development Corporation the assumption was that nonwetting phase relative permeabilities (oil and gas in this instance) were independent of the amount of irreducible water present. I feel this is directionally so at low irreducible water saturations - say, less than 20 %, but not so at higher irreducible water saturations. In my opinion the above equations are better catagorized as normalized permeabilities, k_o^{**} and k_g^{**} and should be multiplied by k_r^o determined from Eq. 13 or Fig. 11. The equations given for unconsolidated sands, well sorted grains were developed from a theoretical capillary pressure curve of packed spheres (like stacked ball bearings). Such a

curve corresponds to a pore size distribution index of infinity ($\lambda = \infty$). The cemented sandstones, oölitic limestones, vugular rocks equations corresponds to the condition of the $1/P_c^2$ vs S_L^* curve being a straight line. This condition is equivalent to $\lambda = 2$. The equations in Table 2 can be obtained from Eqs. 24 - 28 by substituting in the specific conditions outlined above.

Two examples will now be given to illustrate the use of ideas developed in this section. Example C shows a calculation procedure for computing $k_{rw}]_{dr}$, $k_{ro}]_{dr}$, and $k_{rg}]_{dr}$ values by use of Eqs 19 - 23. One would use this procedure when log P_c is not linear with log S_w^* . The data used in the example is the dimensionless J factor* vs S_w curve of the Weber Sandstone, Rangely Field, Colorado, of Fig. 18.(10) Actually, the Rangely curve does produce an acceptal linear plot of log J vs log S_w^* as we shall see in Example D.

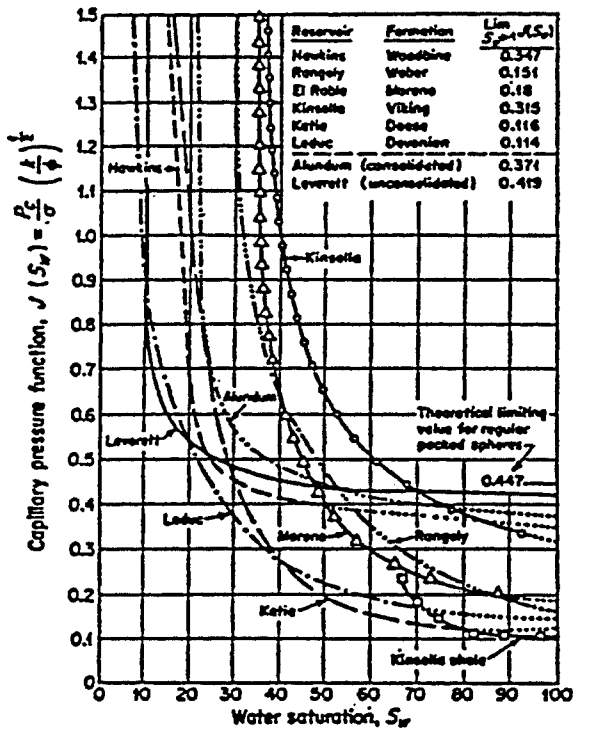

Capillary retention curves. (*From Rose and Bruce.*)[10]

Figure 18

Example C. Calculation of Drainage k_{rw} , k_{ro} , and k_{rg} Values. Weber Sandstone, Rangely Field, Colorado.

Given: Leverett J vs S_w curve, Fig.18

$S_{iw} = 0.30$; $S_w = 0.44$; $S_m = 1.0$

Solution: Step 1. Calculation of S_L^* and $1/J^2$.

S_w	J_{Dim}	$S_L^* \simeq S_w^*$	$1/J_{Dim}^2$
0.35	0.78	0.071	1.64
0.40	0.64	0.143	2.44
0.50	0.48	0.286	4.34
0.60	0.35	0.429	8.16
0.70	0.28	0.571	12.75
0.80	0.23	0.714	18.90
0.90	0.18	0.857	30.86
1.00	0.15	1.000	44.44

$$S_L^* = (S_w - 0.30)/0.70$$

* The Leverett J function can be used in place of P_c in all equations developed so far as J is the product of a constant and P_c. The dimenionless J used in Fig. 18 makes use of metric units, for which P_c = dyne/ cm^2 ; k = cm^2 ; and σ = dyne/cm . If oilfield units of P_c = psi ; k = md. ; and σ = dyne/cm are used to compute J , then

$$J_{Field} = 4.5\, J_{Dim} \qquad (29)$$

Step 2. Calculation of areas under $1/J^2$ vs S_L^* curve.

S_L^* Interval	Area	Cum. Area
0.0-0.1	0.088	0.088
0.1-0.2	0.257	0.345
0.2-0.3	0.412	0.757
0.3-0.4	0.613	1.370
0.4-0.5	0.882	2.252
0.5-0.6	1.202	3.454
0.6-0.7	1.600	5.054
0.7-0.8	2.098	7.152
0.8-0.9	2.820	9.972
0.9-1.0	3.820	13.792

At $S_w = 0.44$

$S_w^* = (0.44-0.30)/0.70 = 0.20$

$\int_0^{S_w^*} dS_I^*/J^2 = 0.345$

At $S_o^* = 0.3 \cong S_L^* = 0.5$

$\int_{S_w^*}^{S_L^*} dS_I^*/J^2 = 2.252 - 0.345 = 1.907$

$\int_0^{1} dS_I^*/J^2 = 13.792$

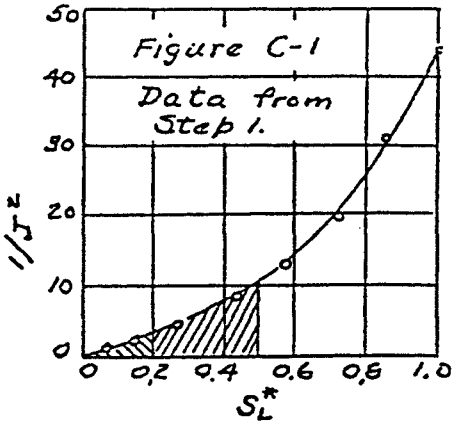

Note: Areas listed in the above tabulation were calculated from a large scale plot like Fig. C-1 and Simpson Rule integration.

Step 3. Calculation of water relative permeability, $k_{rw}]_{dr}$.

$S_w = 0.44$; $S_{iw} = 0.30$; $S_w^* = (0.44-0.30) / (1-0.30) = 0.20$

From Equation 19 -

$$k_{rw}]_{dr} = k_r^o \frac{k_w}{k_w)_{S_w^*=1}} = (S_w^*)^2 \cdot \frac{\int_0^{S_w^*} dS_I^*/J^2}{\int_0^{1} dS_I^*/J^2}$$

(always 1 for "most wetting" phase)

$\therefore k_{rw}]_{dr} = (0.20)^2 \cdot 0.345/13.792 = 0.0010$

Step 4. Calculation of oil relative permeability, $k_{ro}]_{dr}$.

$S_w = 0.44 = S_w^* = 0.20$; $S_{iw} = 0.30$ $k_r^o = 0.623$ (Eq. 13)

From Equation 20 -

$$k_{ro}]_{dr} = k_r^o \cdot \bar{k} = k_r^o \cdot (S_o^*)^2 \cdot \frac{\int_{S_w^*}^{S_L^*} dS_I^*/J^2}{\int_0^{1} dS_I^*/J^2}$$

At $S_o^* = 0.30$; $S_L^* = 0.50$ and $S_o = 0.3 \cdot (1-0.3) = 0.21$

$\therefore k_{ro}]_{dr} = 0.623 \cdot (0.30)^2 \cdot (2.252-0.345)/13.792 = 0.00775$

S_o^*	$\frac{\int_{S_w^*}^{S_L^*} dS_L^*/J^2}{\int_0^{1} dS_L^*/J^2}$	$k_{ro}]_{dr}$	S_o
0.1	0.0299	0.00019	0.07
0.2	0.0743	0.00185	0.14
0.3	0.138	0.00775	0.21
0.4	0.225	0.0225	0.28
0.5	0.341	0.0532	0.35
0.6	0.494	0.111	0.42
0.7	0.698	0.213	0.49
0.8	0.975	0.389	0.56

Step 5. Calculation of gas relative permeability, $k_{rg}]_{dr}$.

$S_w = 0.44$; $S_{iw} = 0.30$ $k_r^o = 0.623$ (Eq. 13) ; $S_m = 1$

From Equation 21 -

$$k_{rg}]_{dr} = k_r^o \cdot k_g^{**} = k_r^o \cdot (S_g^*)^2 \cdot \frac{\int_{S_L^*}^{1} dS_L^*/J^2}{\int_{0}^{1} dS_L^*/J^2}$$

At $S_g^* = 0.30$; $S_L^* = 0.70$ and $S_o^* = 0.50$

$$k_{rg}]_{dr} = 0.623 \cdot (0.30) \cdot (13.792-5.054)/13.792 = 0.0355$$

S_g^*	$\frac{\int_{S_L^*}^{1} dS_L^*/J^2}{\int_{0}^{1} dS_L^*/J^2}$	$k_{rg}]_{dr}$	S_g
0.8	0.975	0.389	0.56
0.7	0.945	0.289	0.49
0.6	0.901	0.202	0.42
0.5	0.837	0.130	0.35
0.4	0.750	0.0747	0.28
0.3	0.634	0.0355	0.21
0.2	0.481	0.0120	0.14
0.1	0.277	0.00173	0.07

Step 6. Summary of calculations.

Field: Rangely, Colorado
Sand: Weber
Data Source: Rose and Bruce (10)

$S_w = 0.44$; $S_{iw} = 0.30$; $S_o + S_g = 0.56$; $S_m = 1$.

S_g	S_o	$k_{rg}]_{dr}$	$k_{ro}]_{dr}$	$k_{rg}/k_{ro}]_{dr}$
0	0.56	0	0.389	0
0.07	0.49	0.00173	0.213	0.00812
0.14	0.42	0.0120	0.111	0.108
0.21	0.35	0.0355	0.0532	0.667
0.28	0.28	0.0747	0.0225	3.32
0.35	0.21	0.130	0.00775	16.8
0.42	0.14	0.202	0.00185	109
0.49	0.07	0.289	0.00019	1520
0.56	0	0.389	0	∞

$$k_{rw}]_{dr} = 0.0010$$

The calculation procedure illustrated above in Example C is quite laborious - primarily because of the graphical integration of the $1/J^2$ vs S_L^* curve. An alternate to the graphical integration is to fit the curve (see Fig. C-1) with a

polynomial equation and perform the integration on the equation.

Example D uses the same capillary pressure - saturation data as Example C. The object here, however, is to illustrate the use of Eqs. 24 - 28 and to compare resulting values with those of Example C and values obtained by use of Wyllie's equations in Table 2.

Example D. Calculation of λ and Drainage k_{rw}, k_{ro}, and k_{rg} Values.
Weber Sandstone, Rangely Field, Colorado.

Given: Leverett J vs S_w curve, Fig.18.
$S_{iw} = 0.30$; $S_w = 0.44$; $S_m = 1$.

Solution: Part 1. Determination of λ.

S_w	J_{Dim}	$S_L^* = S_w^*$
0.35	0.78	0.071
0.40	0.64	0.143
0.50	0.48	0.286
0.60	0.35	0.429
0.70	0.28	0.571
0.80	0.23	0.714
0.90	0.18	0.857
1.00	0.15	1.000

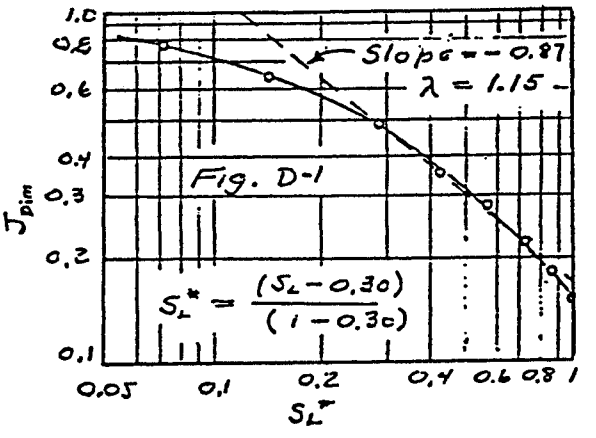

Note that log J is not linear with log S_L^*. A straight line that fits the data in the region $0.29 < S_L^* < 1$ yields a pore size distribution index of 1.15. It is best to fit the high values of S_L^* as this is the range of saturation of interest to gas and oil relative permeabilities.

Part 2. Calculation of $k_{rw}]_{dr}$, $k_{ro}]_{dr}$, and $k_{rg}]_{dr}$ by Eqs. 24, 26, 28.

$\lambda = 1.15$; $S_m = 1$; $S_w^* = 0.20$; $k_r^o = 0.623$; $\frac{2+\lambda}{\lambda} = 2.74$; $\frac{2+3\lambda}{\lambda} = 4.74$

S_g	S_g^*	S_o^*	S_L^*	$(S_L^*)^{2.74}$	$(S_w^*)^{2.74}$	$k_{ro}]_{dr}$	$k_{rg}]_{dr}$	$k_{rg}/k_{ro}]_{dr}$
0	0	0.8	1.0	1.000	0.0122	0.394	0	0
0.07	0.1	0.7	0.9	0.749		0.225	0.00156	0.00693
0.14	0.2	0.6	0.8	0.543		0.119	0.0114	0.0958
0.21	0.3	0.5	0.7	0.376		0.0567	0.0350	0.617
0.28	0.4	0.4	0.6	0.247		0.0234	0.0751	3.21
0.35	0.5	0.3	0.5	0.150		0.00771	0.132	17.12
0.42	0.6	0.2	0.4	0.0812		0.00172	0.206	120
0.49	0.7	0.1	0.3	0.0369		0.000154	0.294	1909
0.56	0.8	0	0.2	0.0122		0	0.394	∞

$k_{rw} = (0.20)^{4.74} = 0.00049$

Part 3. Calculation of $k_{rw}]_{dr}$, $k_{ro}]_{dr}$, and $k_{rg}]_{dr}$ by Wyllie's Eqs.(Table 2)

$S_w = 0.44$; $S_{iw} = 0.30$; $(k_r^o = 0.623)$

Note: The Weber sandstone is a very well consolidated quartzitic sandstone. The lower equation of Table 2 applies.

S_g	S_o	$k_{ro}]_{dr}$	$k_{rg}]_{dr}$	$k_{rg}/k_{ro}]_{dr}$
0	0.56	0.683	0	0
0.07	0.49	0.480	0.00118	0.00247
0.14	0.42	0.320	0.0090	0.0280
0.21	0.35	0.200	0.0286	0.143
0.28	0.28	0.114	0.0638	0.560
0.35	0.21	0.0561	0.117	2.08
0.42	0.14	0.0214	0.188	8.82
0.49	0.07	0.00445	0.278	62.4
0.56	0	0	0.383	∞

$$k_{rw}]_{dr} = (0.20)^4 = 0.0016$$

Part 4. Comparison of Calculated $k_{ro}]_{dr}$, $k_{rg}]_{dr}$, and $k_{rg}/k_{ro}]_{dr}$ Values.

Note: The following tabulation compares relative permeability values calculated in Parts 2 and 3 above with comparable values calculated in Example C. The comparison is on the ratio of values.

	Values by Eqs 26 and 28 / Values by Eqs 20 and 21			Values by Wyllie's Eq. / Values by Eqs 20 and 21		
S_g	$k_{ro}]_{dr}$	$k_{rg}]_{dr}$	$k_{rg}/k_{ro}]_{dr}$	$k_{ro}]_{dr}$	$k_{rg}]_{dr}$	$k_{rg}/k_{ro}]_{dr}$
0	1.013	—	—	1.756	—	—
0.07	1.056	0.902	0.853	2.254	0.682	0.304
0.14	1.072	0.950	0.887	2.883	0.750	0.259
0.21	1.066	0.986	0.925	3.759	0.806	0.214
0.28	1.040	1.005	0.967	5.067	0.854	0.169
0.35	0.995	1.015	1.019	7.239	0.900	0.124
0.42	0.930	1.020	1.101	11.57	0.931	0.081
0.49	0.810	1.017	1.256	23.42	0.962	0.041
0.56	—	1.013	—	—	0.985	—

Comments. It can be seen from the above tabulation that approximating the log J vs log S_L^* curve by the straight line shown in Fig D-1 resulted in errors up to 25% in k_{rg}/k_{ro} values. Wyllie's equations gave large errors in k_{rg}/k_{ro} values (to 2500%). This is because Wyllie's equations apply only to pore size distribution index of 2 whereas the Weber Sandstone used in the example has an index of approximately 1. One should be careful in using Wyllie's equations unless it is known that the pore size distribution index is close to 2.

This concludes the section on developing three-phase drainage relative permeability values from capillary pressure curves. The relationships shown

on page 24 and 25 are very useful when laboratory measured drainage values are not available but drainage capillary pressure curves are available. The next section will develop a theory that can be used to calculate two-phase imbibition relative permeability values.

Theory of Two-Phase Imbibition Relative Permeabilities.

Imbibition relative permeabilities apply when the wetting phase is, or has been, increasing in magnitude. The most important use of imbibition values is in waterflood calculations where water (wetting phase) is displacing oil (non-wetting phase). A similar application of imbibition values occurs in calculations concerned with influx of aquifer water into gas reservoirs.

Laboratory work carried out in the eary 1950 period showed that the direction of saturation change has an important bearing on the value of the non-wetting phase relative permeability at a given saturation. The basic difference in values is illustrated by the two non-wetting phase curves of Fig. 19. As can be seen, the drainage curve has a greater value, at a given saturation , than the imbibition value. On the other hand, apparently there is little difference in drainage and imbibition values for the wetting phase. Therefor, in this section we will be concerned only with the behavior of the non-wetting phase and will develop equations that fit its behavior.

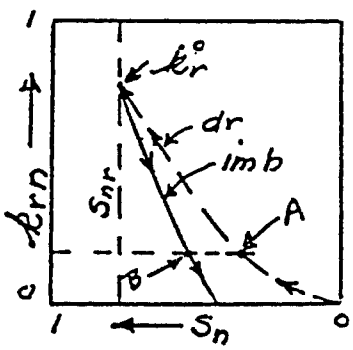

Figure 19

A reasonable explaination for the behavior illustrated in Fig 19 can be developed by considering the difference in behavior when a pore system is being drained of wetting phase and when it is imbibing wetting phase. Under drainage operations capillary forces and viscous forces both operate in a direction that promotes desaturation of the largest pores first, followed by progressive desaturation of smaller and smaller pores. Under imbibition operations, however, capillary forces and viscous forces operate, in effect, in opposite directions. Cappilary forces favor resaturation of the smallest pores first while viscous forces favor resaturation of the largest pores first. The net effect is that pore sizes are not resaturated in the

same sequence during imbibition as they are desaturated during drainage. During the imbibition process a portion of the non-wetting phase becomes trapped by wetting phase and consequently does not contribute to relative permeability. Refering to Fig. 19 , if A represents a relative permeability-saturation value on the drainage curve, the saturation on the imbibition caurve that has the same relative permeability value is indicated by B. The trapped saturation developed during imbibition from $k_r^o : S_{nr}$ to saturation B is the difference in B and A saturation values.

The most important early work on imbibition relative permeability behavior was that of Naar and Henderson (11). The more recent work of C.S.Land of the U.S. Bureau of Mines (12) (13) is of greater importance in that it leads to useful mathematical relationships which apparently are in good agreement with laboratory measurements. The notes that follow essentially reproduce Land's work.

The crux of Land's method of calculating two and three-phase imbibition relative permeability values is to subtract the amount of trapped non-wetting phase saturation from the total non-wetting phase saturation. This yields a "free" saturation value (free to flow and consequently contribute to the relative permeability) that is used in the same basic equations discussed previously for drainage processes. The amount of trapped non-wetting phase depends on the particular rock involved and the number of saturation units in which imbibition takes place.

The material that follows is presented for two phase conditions. The non-wetting phase is indicated by the subscript n and would. correspond to either gas or oil phase in a petroleum reservoir. The wetting phase is indicated by the subscript w and normally would be considered to correspond to water phase in a reservoir. As indicated above the trapping characteristic of the rock is an important addition to previous theory so it will be discussed first.

Trapped Non-Wetting Phase Saturation. Imbibition experiments with core samples show that the residual non-wetting phase saturation , S_{nr} , that is finally attained as a result of imbibition is related to the initial non-wetting phase saturation, S_{ni} , and some characteristic of the core. Land (12) found that a general relationship could be written in terms of effective saturations as

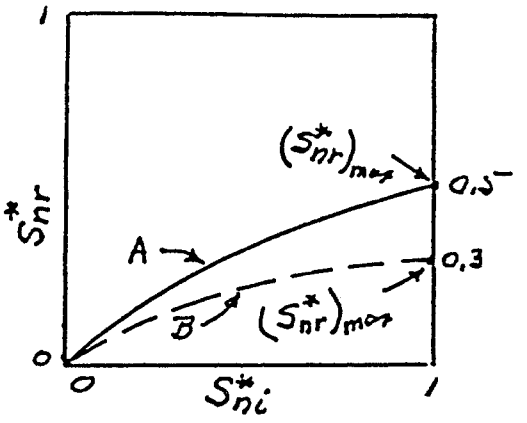

Figure 20

$$1/S^*_{nr} - 1/S^*_{ni} = C \qquad (30)$$

where C is a " trapping constant" of the rock. The effective saturations are, of course expressed as

$$S^*_{ni} = S_{ni} / (1 - S_{iw}) \qquad (31)$$

$$S^*_{nr} = S_{nr} / (1 - S_{iw}) \qquad (32)$$

Figure 20 shows shows the characteristics of curves of Eq. 30.

The value of C for a given rock can be determined by simple laboratory experiments. In Fig 20, $S^*_{ni} = 1$ represents imbibition starting from an irreducible wetting phase saturation condition, and $(S^*_{nr})_{max}$ represents the resulting residual non-wetting phase saturation. From Eq. 30

$$C = 1 / (S^*_{nr})_{max} - 1 \qquad (33)$$

Thus to determine C, the rock sample is first saturated 100 % with wetting phase (water, say) , desaturated to irreducible wetting phase saturation by use of capillary pressure equipment, and then allowed to spontaneously imbibe wetting phase to equilibrium. The residual non-wetting phase is then determined and used in Eq. 33 to calculate C.

By way of illustration, the two curves of Fig. 20 have the following trapping constants :

Curve	$(S^*_{nr})_{max}$	C
A	0.5	1.0
B	0.3	2.33

Note that if no trapping occurs (this will be $S^*_{nr} = 0$) the value of C becomes infinity. It is somewhat unfortunate, in my opinion, that Land elected to define the trapping constant such that the higher the value the less residual phase results. It would have been easier to have the relationship the other way around.

In the absence of laboratory results to determine the trapping constant it is probably best to use a value between 1 and 3 in the equations that follow. The value of 3 corresponds to an often used rule of thumb in waterflood calculat-

ions that the residual oil left in a core after many pore volumes of water throughput will be about 20 % of the initial oil saturation at the start of displacement.

The trapping constant, C, is an important parameter in imbibition relative permeability relationships developed in the next section. When one specifies the value of C, he automatically fixes the shape of the non-wetting phase curve.

Imbibition Relationships, Non-Wetting Phase. Relative permeability - saturation equations are usually written in terms of wetting phase saturation units. Thus an expression for the drainage non-wetting phase relative permeability is :

$$k_{rn}]_{dr} = k_r^o \left(1 - S_w^* \right)^2 \left[1 - (S_w^*)^{\frac{2+\lambda}{\lambda}} \right] \qquad (34)$$

(This is also Eq. 12 on page 14). However , there is some slight advantage in writting the present development in terms of non-wetting phase saturation units. Recognizing that in a two-phase system $S_w^* + S_n^* = 1$, Eq. 34 can be restated as

$$k_{rn}]_{dr} = k_r^o \left(S_n^* \right)^2 \left[1 - \left(1 - S_n^* \right)^{\frac{2+\lambda}{\lambda}} \right] \qquad (35)$$

The relationship for the imbibition situation is similar to Eq 35 but differs in that "free" non-wetting phase saturations units are used. This leads to

$$k_{rn}]_{imb} = k_r^o \left(S_{nF}^* \right)^2 \left[1 - \left(1 - S_{nF}^* \right)^{\frac{2+\lambda}{\lambda}} \right] \qquad (36)$$

To use Eq.36 requires that the "free" saturation be known at various values of total non-wetting phase saturation. To accomplish this we can say, first , that total non-wetting phase saturation is the sum of "free" saturation and trapped saturation. That is:

$$S_n^* = S_{nF}^* + S_{nt}^* \qquad (37)$$

A second relationship is that the trapped saturation, at any total non-wetting phase saturation , is equal to the residual non-wetting phase saturation present when $k_{rn}]_{imb} = 0$ minus the amount of non-wetting phase that gets trapped during saturation change from S_n^* to S_{nr}^* . An expression of this behavior is

$$S^*_{nt} = S^*_{nr} - \frac{S^*_{nF}}{CS^*_{nF} + 1} \qquad (38)$$

Eliminating S^*_{nt} between Eqs. 37 and 38 results in a quadratic equation for S^*_{nF}. The solution of the quadratic on interest is

$$S^*_{nF} = 1/2 \left[(S^*_n - S^*_{nr}) + \sqrt{(S^*_n - S^*_{nr})^2 + \frac{4}{C}(S^*_n - S^*_{nr})} \right] \qquad (39)$$

Equation 39 is not in optimum form as it contains the residual non-wetting phase saturation term S^*_{nr}. However, this term can be gotten rid of by solving Eq. 30 for S^*_{nr} and substituting it in Eq. 39. That is, from Eq.30

$$S^*_{nr} = S^*_{ni} / (C S^*_{ni} + 1) \qquad (40)$$

This would yield an equation for the "free" non-wetting phas saturation in terms of the saturation value at the start of the imbibition process, S^*_{ni}, and the existing non-wetting phase saturation, S^*_n. In practice, however, it is easier to employ the two equations separately. That is, use equation 40 to evaluate S^*_{nr} and then plug the value into Eq. 39 to get S^*_{nF}. The resulting value of S^*_{nF} can then be used in Eq. 36 to obtain the imbibition non-wetting phase relative permeability.

Before working an example problem to illustrate the use of Eqs. 40, 39, and 36 in calculating an imbibition curve for a non-wetting phase it is interest to show graphically what the equations infer. Figure 21 shows three imbibition <u>normalized</u> permeability curves, A, B, and C. The corresponding drainage curve is shown as the dashed curve. The starting point of each imbibition curve lies on the drainage curve, as indicated by the small dots. At the starting points there is, of course, no trapped non-wetting phase (because trapping occurs only during the imbibition process and it hasn't started yet) so the relative permeability can be calculated from

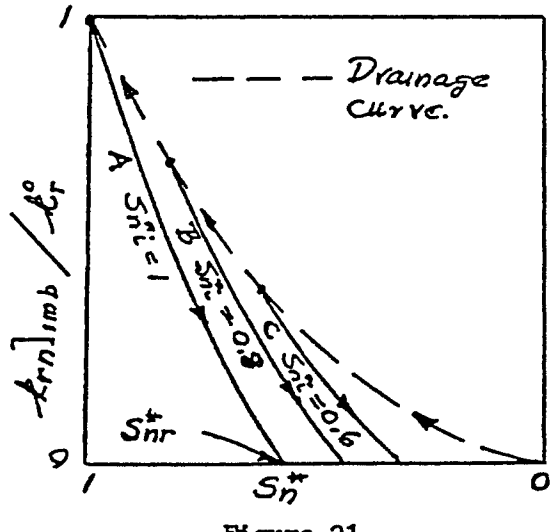

Figure 21

Eq. 36 by noting that $S^*_{nF} = S^*_{ni}$. Or, as the starting points of imbibition curves lie on the drainage curve.Eq. 35 may be used to calculate the relative permeability at the starting point.

The bottom end of an imbibition curve is fixed by the starting saturation, S^*_{ni} , and the trapping constant C in accordance with Eq. 40 . This defines the residual non-wetting phase saturation, S^*_{nr} , the saturation at which $k_{rn}]_{imb} = 0$. Note that as C in Eq 40 increases the value of S^*_{nr} decreases so that the bottom end of the imbibition curve moves to the right in Fig. 21. For a value of C equal to infinity the imbibition curve will lie exactly on the drainage curve.

The shape of the imbibition curves between the two limits is controlled by Eqs. 39 and 36. In general, the lower the value of C the straighter will be the imbibition curve.

The non-wetting phase imbibition relationships developed above consider that no " critical " saturation exists for the drainage curve: that is, the drainage relative permeability curve starts from $S^*_n = 0$ as illustrated in Fig.21. However, should the drainage curve start from some so-called "critical" saturation value, S^*_{nc}, it may be appropriate to introduce a modification into the imbibition equations to account for this. Otherwise, at large values of C the calculated value of $k_{rn}]_{imb}$ may be greater than $k_{rn}]_{dr}$. It will be recalled that for drainage curves the "critical" saturation effect was taken care of by introducing the parameter S_m into the appropriate equations. S_m was defined as the wetting phase saturation at which the non-wetting phase relative permeability curve started. (This is discussed on page 17, and handled by Eq. 18) M.R. Monroy of Chevron Oil Field Research Company (14) has suggested that to handle "critical" saturation effects on non-wetting phase imbibition relationships that Eq. 36 be altered to

$$k_{rn}]_{imb} = k^o_r \left[\frac{(S_m - 1)}{(S_m - S_{iw})} + S^*_{nF} \frac{(1 - S_{iw})}{(S_m - S_{iw})}\right]^2 \left[1 - \left(1 - S^*_{nF}\right)^{\frac{2+\lambda}{\lambda}}\right] \qquad (41)$$

An example calculation of $k_{rn}]_{imb}$ will now be given to illustrate the use of the imbibition equations developed in this section. Example E is based on the Leverett J vs S_W curve of the Viking Formation, Kinsella Reservoir of Fig. 18 , page 29. Oil is assumed to be the non-wetting phase in these calculations. It is also assumed that the irreducible water saturation in

this reservoir is 0.36 and that the actual water saturation is 0.50 at the start of the imbibition process.

Example E. Calculation of λ and Imbibition k_{ro} Values

Viking Formation, Kinsella Reservoir

Given: Leverett J vs S_w curve, Fig 18, page 29.
$S_{iw} = 0.36$; $S_w = 0.50$; $S_m = 1$

Solution: Part 1. Determination of λ.

S_w	$J_D$im	S_w^*
0.40	1.0	0.
0.50	0.65	0.22
0.60	0.52	0.38
0.70	0.44	0.53
0.80	0.37	0.69
0.90	0.35	0.84
1.00	0.32	1.00

$S_w^* = (S_w - 0.36)/(1-0.36)$

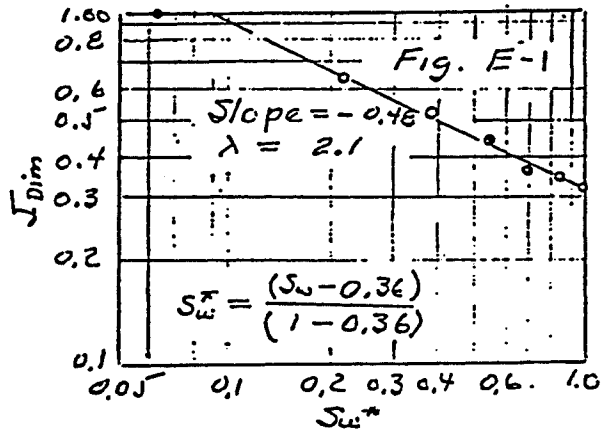

From the slope of the line of Fig E-1, λ is 2.1

Part 2. Calculation of $k_{ro}]_{imb}$ by Equations 40, 39, and 36

$\lambda = 2.1$; $S_{iw} = 0.36$; $S_{wi} = 0.50$; $k_r^o = 0.51$; $C = 1.5$

$(2+\lambda)/\lambda = 1.95$; $S_{oi}^* = 0.5/(1-0.36) = 0.781$

$S_{or}^* = S_{oi}^*/(C\, S_{oi}^* + 1) = 0.781/(1.5 \cdot 0.781 + 1) = 0.360$

$$S_{oF}^* = 1/2 \left[(S_o^* - S_{or}^*) + \sqrt{(S_o^* - S_{or}^*)^2 + \frac{4}{C}(S_o^* - S_{or}^*)} \right] \qquad (1)$$

S_o	S_o^*	$(S_o^* - S_{or}^*)$	S_{oF}^*	$(S_{oF}^*)^2$	$(1-S_{oF}^*)^{1.95}$	$k_{ro}]_{imb}$	$k_{ro}]_{dr}$
0.50	0.781	0.421	0.781	0.609	0.0519	0.295	0.295
0.45	0.703	0.343	0.680	0.462	0.109	0.210	0.228
0.40	0.625	0.265	0.573	0.329	0.190	0.136	0.170
0.35	0.547	0.187	0.459	0.210	0.302	0.075	0.120
0.30	0.469	0.109	0.330	0.109	0.459	0.030	0.079
0.25	0.391	0.031	0.160	0.0256	0.712	0.004	0.048
0.23	0.360	0.000	0.000	0.0000	1.000	0.000	0.038

(1) Drainage values calculated from Eq. 12 for comparison with $k_{ro}]_{imb}$

Imbibition Relationships, Wetting Phase. In two-phase systems the amount of wetting phase over and above the irreducible value is mobile and contributes to relative permeability. During imbibition, as the wetting phase saturation increases from its initial value some non-wetting phase is trapped. This trapping behavior was explained previously on page 35. As a result of non-wetting phase entrapment the wetting phase occupies pores of larger size, at a given saturation, than it would have occupied had entrappment not occured. As fluids flow easier in large pores than in small pores, the effect of the entrapment is to yield a larger value of relative permeability. Thus, directionally the imbibition relative permeability curve should lie above the drainage curve as illustrated in Fig. 22. On the other hand, it can be argued that entrappment of non-wetting phase should result in a slightly longer flow path for the wetting phase - which would act towards decreasing the imbibition relative permeability.

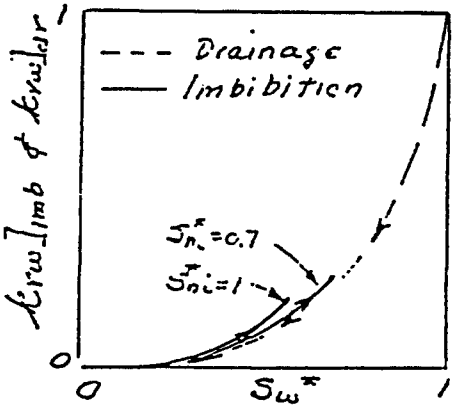

Figure 22

Relatively simple equations for calculating the effect of trapping non-wetting phase during imbibition have not been worked out. Land (12) showed for one specific set of conditions ($\lambda = 2$; $C = 1.5$) that in most of the saturation range of interest there was little difference between the imbibition and drainage curves. Until further developments on this point are presented it seems best to assume that the two curves are the same. The appropriate equtions are:

$$k_{rw}]_{imb} = k_{rw}]_{dr} = (S_w^*)^{\frac{2+3\lambda}{\lambda}} \qquad (42)$$

or

$$k_{rw}]_{imb} = k_{rw}]_{dr} = (1 - S_n^*)^{\frac{2+3\lambda}{\lambda}} \qquad (43)$$

Calculation of $k_{rw}]_{imb}$ values from either Eq. 42 or 43 is straight forward. Example F illustrates the calculation based on the Leverett J vs S_w curve of the Viking Formation, Kinsella Reservoir of Fig. 18, page 29. As in Example E, it is assumed that irreducible water in this reservoir is 0.36 and that the actual water saturation is 0.50 at the start of the imbibition.

Example F. Calculation of Imbibition k_{rw} Values

Viking Formation, Kinsella Reservoir

Given: Leverett J vs S_w curve, Fig. 18, page 29.
$S_{iw} = 0.36$; $S_{wi} = 0.50$; $S_m = 1$; $\lambda = 2.1$ (From Ex. E)

Solution:

$$(2 + 3\lambda)/\lambda = 3.95 \; ; \; k_{rw}]_{imb} = (1 - S_o^*)^{3.95}$$

S_o	S_o^*	$(1 - S_o^*)$	$k_{rw}]_{imb}$	$k_{rw}/k_{ro}]_{imb}$ (1)
0.50	0.781	0.219	0.0025	0.0083
0.45	0.703	0.297	0.0083	0.039
0.40	0.625	0.375	0.021	0.153
0.35	0.547	0.453	0.044	0.584
0.30	0.469	0.531	0.082	2.74
0.25	0.391	0.609	0.141	37.6
0.23	0.360	0.640	0.172	∞

(1) Imbibition k_{ro} values from Example E.

NOMENCLATURE

C	trapping constant characteristic of each porous media $= 1/(S^*_{nr})_{max} - 1$
J	Leverett J function
k	absolute permeability
k_a	air permeability
k_g	effective permeability to gas
k_o	effective permeability to oil
k_w	effective permeability to water
k_n	effective permeability to a non-wetting phase
k_w	effective permeability to a wetting phase
k_{rg}	relative permeability to gas, $= k_g / k$
k_{ro}	relative permeability to oil, $= k_o / k$
k_{rw}	relative permeability to water $= k_w / k$
$k_w)_{S_w=1}$	effective wetting phase permeability at wetting phase saturation equal to 1.
$k_n)_{S_w=0}$	effective non-wetting phase permeability at wetting phase saturation equal to 0.
k^{**}_w	normalized wetting phase permeability $= k_w / k_w)_{S_w=1}$
k^{**}_n	normallized non-wetting phase permeability $= k_n / k_n)_{S_w=0}$
k^o_r	relative permeability of non-wetting phase(s) at irreducible wetting phase saturation $= k_n)_{S_{iw}} / k$
λ	(lambda) pore size distribution index , exponent in equation $P_e / P_c = (S^*_w)^\lambda$
P_e	capillary entry pressure
P_c	capillary pressure
ϕ	porosity
S	saturation,
S_{gr}	residual gas saturation
S_{gF}	"free" (mobile) gas saturation
S_{gt}	trapped gas saturation
S_{nr}	residual non-wetting phase saturation
S_{nF}	"free" (mobile) non-wetting phase saturation
S_{nt}	trapped non-wetting phase saturation
S_o	oil saturation
S_{or}	residual oil saturation

NOMENCLATURE (Continued)

S_w	water saturation
S_w	wetting phase saturation
S_{iw}	irreducible water or wetting phase saturation
S_{wi}	initial water of wetting phase saturation
S_m	total liquid phases saturation at start of non-wetting phase relative permeability curve. $= 1 - S_{cn}$
S_{cn}	critical non-wetting phase saturation (usually gas)
S^*	effective saturation
S_g^*	$= S_g / (1 - S_{iw})$
S_o^*	$= S_o / (1 - S_{iw})$
S_w^*	$= (S_w - S_{iw})/(1 - S_{iw})$
S_n^*	$= S_n / (1 - S_{iw})$
S_{nF}^*	$= S_{nF} / (1 - S_{iw})$
σ	(sigma) interfacial tension

Subscripts

F	free or mobile
dr	drainage cycle (decreasing wetting phase saturation)
imb	imbibition cycle (increasing wetting phase saturation)

REFERENCES

1. Fatt, I. "The Network Model of Porous Media " I, II, III Trans AIME (1956) 207, 144-177

2. Brooks, R.H. and Corey, A.T. " Hydraulic Properties of Porous Media " Hydraulic Paper No 3, Colorado State University, 1964

3. Brooks, R.H. and Corey, A.T. " Properties of Porous Media Affecting Fluid Flow " Jour. of the Irrigation and Drainage Division, Proc. of ASCE (1966) No IR 2, 61-88

4. Burdine, N.T. " Relative Permeability Calculations from Pore Size Distribution Data " Trans AIME (1953) 198, 71-78.

5. Wylie, M.R.J. " Relative Permeability " Petroleum Production Handbook, Chapter 25, Vol II, McGraw-Hill Publishers, 1962

6. Corey, A.T. and Rathjens, C.H. " Effect of Stratification on Relative Permeability " Trans AIME (1956) 207, 353

7. Johnson, C.E. " A Two-Point Graphical Determination of the Constants S_{Ir} and S_m in the Corey equation for Gas-Oil Relative Permeability Ratio " Journal of Petroleum Technology, October 1968.

8. Corey, A.T., Rathjens, C.H., Henderson, J.H., and Wylie, M.R.J. "Three-Phase Relative Permeability " Trans AIME (1956) 207, 349

9. Wyllie, M.R.J. and Gardener, G.H .F. " The Generalized Kozeny-Carman Equation: Its Application to Problems of Multiphase Flow in Porous Media " World Oil, March and April 1958

10. Rose, Warter and Bruce, W.A. " Evaluation of Capillary Character in Petroleum Reservoir Rock." Trans AIME (1949) 186, 127 Figure 18 was reproduced from page 156 of Amyx, Bass, and Whiting's Petroleum Reservoir Engineering, McGraw-Hill Book Company, 1960 ed.

11. Naar, J. and Henderson, J.H. " An Imbibition Model - Its Application to Flow Behavior and the Prediction of Oil Recovery "Trans AIME (1961) 222, 61

12. Land, C.S. " Calculation of Imbibition Relative Permeability for Two- and Three-Phase Flow from Rock Properties " Trans AIME (1968) 243, 149

13. Land, C.S. " Comparison of Calculated with Experimental Imbibition Relative Permeabity " Trans AIME (1971) 251, 419

14. Private communication. M.R.Monroy , Chevron Oil Field Research Co.

Problem B-1 — Calculation of Reservoir Capillary Pressures

(The purpose of this simple exercise is to illustrate the calculation of capillary pressures and capillary pressure gradients in reservoirs.)

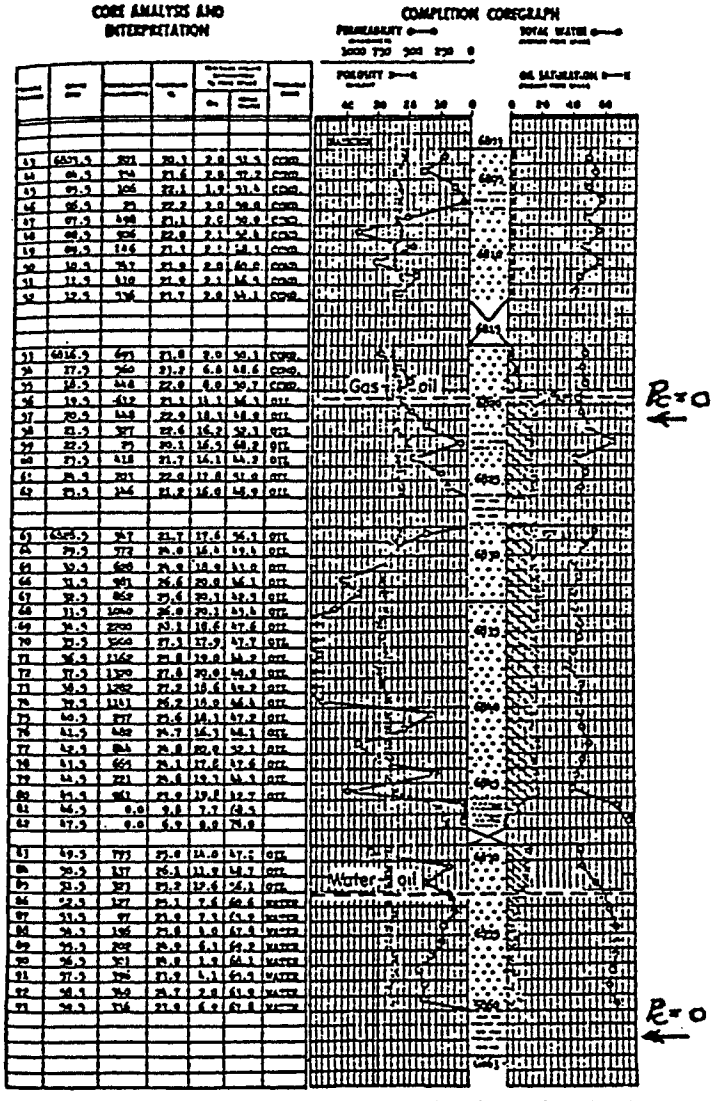

Fig. 7-24. Core log of an oil-producing formation illustrating selection of gas-oil and water-oil contacts. (*From Core Laboratories, Inc.*)

521

The Core Labs completion coregraph at the left shows two transition zones. The gas-oil transition lies between 6816 and 6820 feet. The oil-water transition zone starts at about 6850 but its lower limit is somewhat indefinitely defined.

Elevations at which $P_c = 0$ are always below the corresponding transition zone. For this problem we will consider that $P_c = 0$ at 6821 (gas-oil) and at 6862 (oil-water).

The depth of this formation and usual hydrostatic pressure and temperature gradients indicate that initial pressure/temperature conditions at this location to be near 3000 psig and 200 °F. At these conditions the reservoir fluid densities should be close to

connate water = 65.0 lb/ft^3
oil (gas sat) = 41.0 lb/ft^3
gas-cap gas = 12.0 lb/ft^3

Use these values in your calculations.

What's Wanted

(1) The numerical value of the capillary pressure at 6803.5 feet (core # 43).

(2) Rate of change of capillary pressure with depth in the gas cap and oil band sections of the reservoir.

Answers

(1) 13.27 psi
(2) 0.368 psi/ft ; 0.167 psi/ft.

Solution Problem B-1.

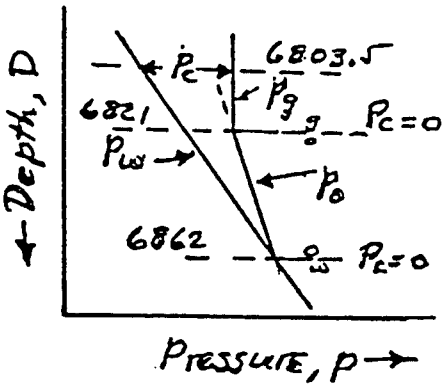

Capillary pressure gradient in oil band $= \frac{(P_w - P_c)}{144}$ psi/ft

$= \frac{(65.0 - 41.0)}{144} = 0.167$ psi/ft

Capillary pressure gradient in gas cap $= \frac{(P_w - P_c)}{144}$ psi/ft

$= \frac{(65.0 - 12.0)}{144} = 0.368$ psi/ft.

$$P_c\Big]_{g/w}^{6803.5} = (6862 - 6821) \cdot 0.167 + (6821 - 6803.5) \cdot 0.368$$

$$= 6.83 + 6.44 = 13.29 \text{ psi.}$$

1) 13.27 psi.

2) $\left(\frac{\Delta P_c}{\Delta D}\right)_{gas/oil} = 0.368$ psi/ft

$\left(\frac{\Delta P_c}{\Delta D}\right)_{oil} = 0.167$ psi/ft.

Problem B-2

Development of a Leverett J Function - Water Saturation Curve from Laboratory Capillary Pressure Data.

(The primary purpose of converting laboratory measured P_c - S_w data to Leverett J function - S_w data is to obtain a single relationship from which water saturation in the reservoir can be estimated at any given elevation for any given fluid pairs, and any given permeability-porosity combination. Basically, the J function represents a means of normalizing laboratory values into relationships (plots or equations) easily used in reservoir calculations. Putting capillary pressure data into J form is a means of detecting erroneous data (yes, laboratories do turn out some) or non-conforming data.)

The following data are a portion of the capillary pressure - saturation data measured on 14 cores from a sandstone reservoir in California. (Only three sets of data are given in order to shorten up the problem) The tests were run by displacing filtered formation brine by kerosene (a very poor practice). For this problem we will assume that the interfacial tension, σ , was 42 dynes/cm and that the oil-water contact angle, θ , was 60° in the laboratory tests.

Assignment

Calculate values of the Leverett J function corresponding to each of the given saturation values. Plot log J vs S_w (three-cycle semi-log paper) and construct what you believe to be the best average curve through the points. Take care in making the plot as it will be used in several other problems.

Laboratory Data

Sample	k_{air} md	ϕ %	Capillary Pressure - psi 0.5	1.0	1.5	2.0	3.0	4.0
			Water Saturation, S_w - %					
5	115	19.0	89.5	60.0	47.8	43.1	38.1	35.1
28	581	20.0	68.0	45.0	37.5	34.4	31.3	29.4
18	1640	27.0	65.0	36.4	33.2	31.1	28.3	26.9

	5.0	6.0	7.0	8.0
5	33.1	31.8	30.9	30.0
28	28.2	27.6	27.4	27.4
18	25.7	24.9	24.2	23.8

Solution Problem B-2.

$$J = \frac{P_c \cdot \sqrt{k/\phi}}{6 \cos\theta}$$; for this problem.

$$\therefore J = \frac{psi\sqrt{md/fract}}{21}$$

P_c = psi
k = md
ϕ = fraction
6 = dynes/cm = 42
$\cos\theta = \cos 60° = 0.5$

Sample	k_{air}	ϕ_{frac}	Capillary Pressure, psi					
			0.5	1.0	1.5	2.0	3.0	4.0
			J Functions					
5	115	0.19	0.59	1.17	1.75	2.34	3.51	4.69
25	561	0.20	1.25	2.57	3.85	5.13	7.70	10.27
15	1640	0.27	1.86	3.71	5.57	7.42	11.13	14.85

	5.0	6.0	7.0	8.0
5	5.86	7.03	8.20	9.37
25	12.83	15.40	17.97	20.53
15	18.56	22.27	25.98	29.69

See plot for values.

Problem B-2 Page 2.

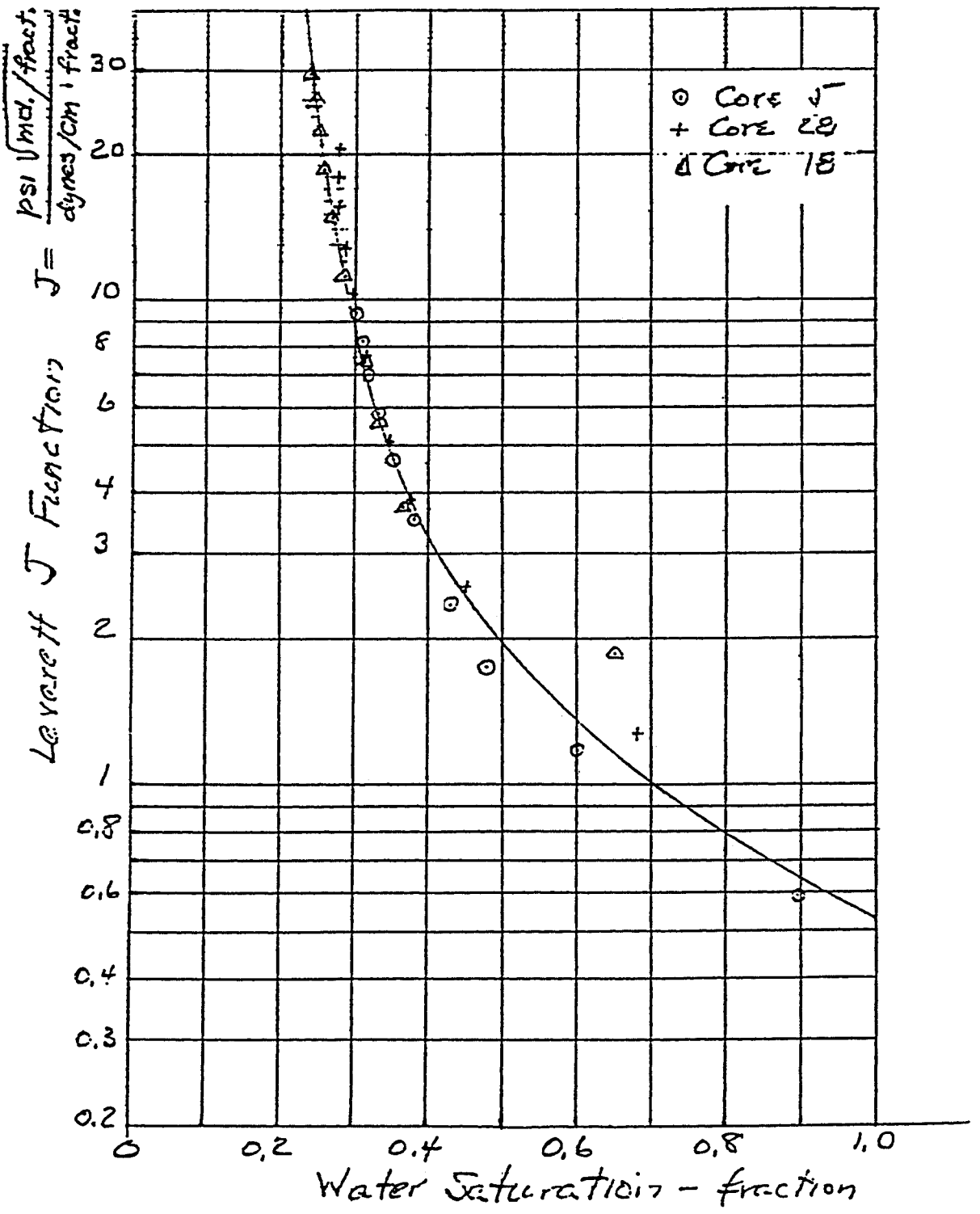

Ans.

Problem B-3

Use of Leverett J Function and Reservoir Parameters to Calculate Average Water Saturation of a Given Section of Reservoir.

(One important use of $J - S_w$ correlations is in evaluating an average water saturation of a given section of reservoir. This problem illustrates the procedure involved.)

In this problem you are to calculate the best possible value for the average connate water saturation, S_{wc} , of the gas cap interval shown in Core Labs' completion coregraph of Problem B-1. In doing this you are to assume that the J function - S_w curve developed in Problem B-2 is applicable to this reservoir. You may neglect in you calculations the three feet of lost core shown in the interval 6813 - 6816. Reservoir fluid properties that might be involved in your calculations are:

Pressure, psig	= 3000 psig
Temperature, °F	= 200
Water density, pcf	= 65.0
Oil density, pcf	= 41.0
Gas density, pcf	= 12.0
Connate water salinity, ppm.	= 65,000

Answer

$$\overline{S_{wc}}\Big|_{6621}^{6803} = 28.7\ \%$$

Solution Problem B-3.

Given: (1) J vs S_w curve of B-2 (2) P, T, ρ data, (2) Correlograph of Prob. B-1

Solution:

From interfacial tension chart $\sigma_{CH_4/brine} = 34 + 2.3 = 36.3$ dynes

Assume $\theta = 0$ in gas cap.

Case = 1

Let ΔD = depth of calc. below 6800 ft.

$$J(D) = \frac{P_c\sqrt{k/\phi}}{\sigma \cos\theta} = \frac{P_c\sqrt{k/\phi}}{36.3}$$

P_c @ 6800 ft = $(6862-6821)\frac{(61.0-41.0)}{144} + (6821-6800)\frac{(61.0-15.}{144}$

$= 6.85 + 7.73 = 14.56$ psi

$$P_c(D) = 14.56 - 0.368\,\Delta D$$

$$\therefore J(D) = \frac{(14.56 - 0.368\,\Delta D)\sqrt{k/\phi}}{36.3}$$

Depth	ΔD	k	φ	J(D)	S_{wc}(D)
6803.5	3.5	201	0.203	11.50	0.250
6804.5	4.5	354	0.236	13.77	0.270
6805.5	5.5	106	0.221	7.56	0.307
6806.5	6.5	25	0.222	3.56	0.387
6807.5	7.5	495	0.231	15.09	0.267
6808.5	8.5	906	0.220	20.21	0.250
6809.5	9.5	146	0.223	7.63	0.307
6810.5	10.5	747	0.229	16.47	0.263
6811.5	11.5	410	0.219	12.31	0.277
6812.5	12.5	536	0.237	13.05	0.272
6816.5	16.5	693	0.235	12.62	0.277
6817.5	17.5	560	0.232	10.99	0.293
6818.5	18.5	448	0.220	9.60	0.297
6819.5	19.5	612	0.231	10.47	0.285
6820.5	20.5	448	0.229	8.55	0.300
					4.311

$$\overline{S_{wc}} = \frac{4.311}{15} = 0.287$$

Good Landing

Solution Problem B-3.

An alternate is to fit an equation to the J factor curve and solve for $S_{wc}(D)$ directly. For example, in this problem the J factor runs from 3.56 to 20.21. In this range a polynomial fit equation is

$$S_{wc} = 0.614 - 0.506 \log J + 0.1752 (\log J)^2$$

from which $\bar{S}_{wc}$ calculates to be 0.253

Problem B-4. Calculation of Field Average Water Saturation Using Leverett J Function - S_w Correlations Plus Other Reservoir Parameters.

(Calculation of the average water saturation of a reservoir as a whole requires consideration of the reservoir structure as well as pertinate fluid and rock properties. This problem tries to emphasize the effect of structure and is, admittedly , somewhat idealized. Actual situations are more complicated.)

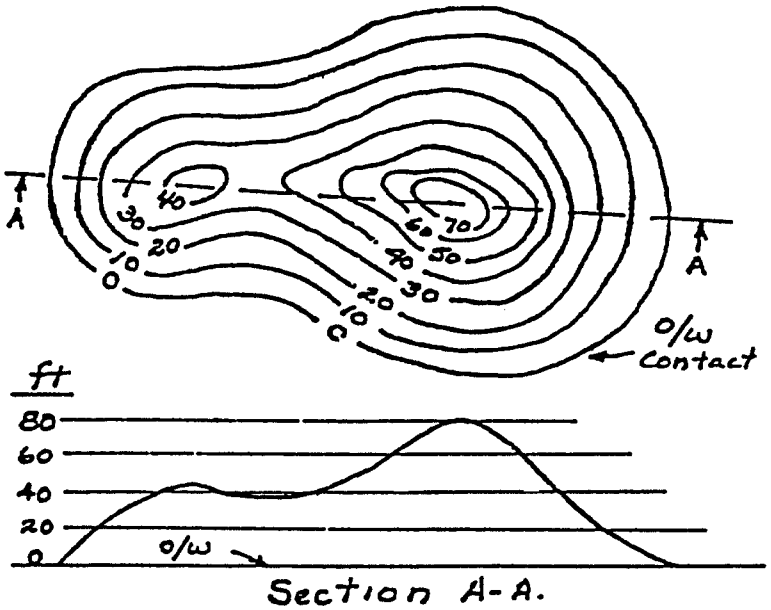

Contour	Acres Enclosed
0	1560
10	1130
20	813
30	534
40	285
50	145
60	71
70	26
80	0

The contour map and cross section shown above illustrates an oil column underlayen by water. For purposes of this problem, we will consider that the oil-water contact is defined as the elevation where capillary pressure is equal to the entry pressure value of the rock-fluids system - not where $P_c = 0$. This is equivalent to saying that only water resides below the oil-water contact. In calculating a value for $\bar{S}_w$ for this reservoir we will also assume that the J - S_w curve developed in Problem B-2 is applicable and that other pertinent reservoir properties are as follows :

Connate water density	= 65 lb/ft^3
Reservoir oil density	= 45 lb/ft^3
Average air permeability	= 100 md
Average porosity	= 20 %
Interfacial tension (O-w)	= 35 dynes/cm
Oil-water contact angle	= 30°

Answer

$$\bar{S}_{wi}\Big|_{o/w}^{o/w\ +80} = 54\ \% \blacksquare$$

Solution Problem B-4.

From J vs S_w curve of Prob. B-3, $J_{antrg} = 0.53$

Let h = feet above oil-water contact

$$J(h) = \frac{h \cdot (\rho_w - \rho_o)}{144} \cdot \frac{\sqrt{k/\phi}}{6 \cos\theta} + 0.53$$

$$= \frac{h\,(65 - 45)}{144} \cdot \frac{\sqrt{100/0.20}}{35 \cdot 0.867} + 0.53$$

$$= 0.1023 \cdot h + 0.53$$

Contour	Area	h	J(h)	S_w(J) From Curve	$S_w \cdot A$
C	1560	0	0.53	1.000	1560
10	1130	10	1.55	0.560	633
20	813	20	2.58	0.440	358
30	536	30	3.60	0.385	206
40	285	40	4.62	0.352	100
50	145	50	5.65	0.330	48
60	71	60	6.67	0.315	22
70	26	70	7.69	0.305	8
80	0	80	8.71	0.297	0

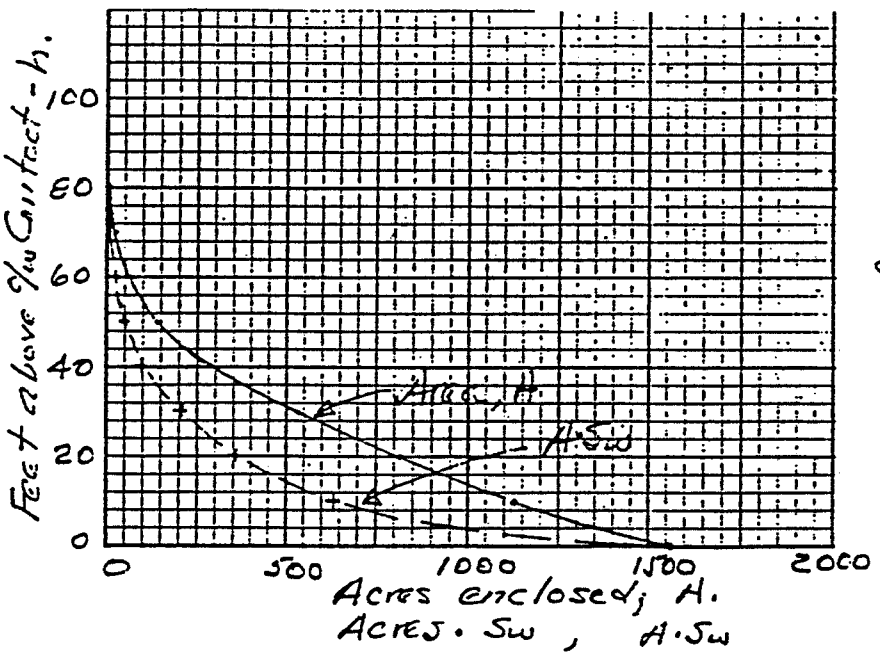

By Simpson Rule Integration

$$\int_0^{80} S_w \cdot A \, dh = 20333$$

$$\int_0^{80} A \cdot dh = 37460 \text{ Acre}$$

$$\bar{S}_w = \frac{20\,333}{37\,460} = 0.54$$

Ans.

Outstanding

Problem B– 5. Development of Drainage Relative Permeability Curves from Capillary Pressure Data.

(Calculating expected oil producing rates, producing gas-oil ratios, and percent recovery of gas and oil during depletion drive (solution drive) operations requires drainage relative permeability - saturation data for the reservoir gas and oil. Other appropriate data are needed also. The purpose of this problem is to show you how easy it is to develop a set of k_{rg} and k_{ro} values from capillary pressure data.)

For this problem we will assume that the oil zone section between shales at 6828 and 6846 on the Core Labs' completion coregraph will be perforated for production. We will also assume that the Leverett J vs S_w curve you developed from the capillary pressure data in Problem B - 2 applies to this reservoir. Other information developed from the coregraph and capillary pressure data that may be pertinent to this problem are :

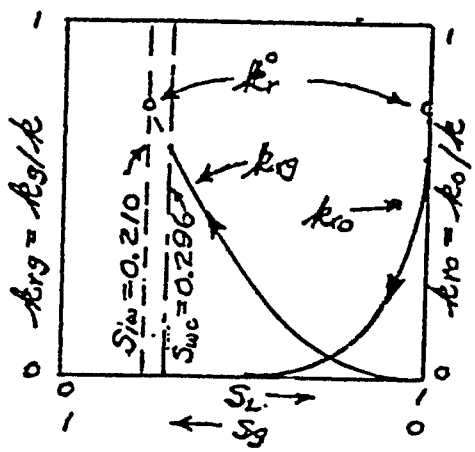

1. The irreducible water saturation for this rock is 21 %.

2. The average water saturation of the oil zone (6828 - 6846) as calculated core-to-core with the J function curve is 29.6 %

3. The geometric average air permeability of the oil zone calculates to be 816 md.

What's Wanted

1. A plot of k_{rg} and k_{ro} vs S_L and S_g as illustrated above. The plot should be on 8½ x 11 inch cordinate paper and indications given of S_{iw} and S_{wc}. Also indicate on the plot the value of k_r^o . You may assume any value desire (within reason) for a critical gas saturation, but indicate its value on the plot.

2. Calculate the effective permeability of gas, oil, and water in the zone when 15 % gas saturation has developed as a result of production.

Answers

1. $\lambda = 0.77$
2. $k_g = 12.6$; $k_o = 152$; $k_w = 0.0033$ md

Solution Problem B-5

Given: (1) J vs S_w plot of problem B-2
(2) $S_{iw} = 0.21$ (4) $k_{ag} = 816$ md.
(3) $\bar{S}_{wc} = 0.296$

Solution:

(1) Determination of λ from J factor plot.

From pg 9 of Rel. Perm notes:

$$(P_c/P_e)^{-\lambda} = S_w^* = \frac{S_w - S_{iw}}{1 - S_{iw}} \quad (1)$$

$$\log P_c = \log P_e - \tfrac{1}{\lambda} \log S_w^* \quad (2)$$

or $$\log J = \log \bar{J}_e - \tfrac{1}{\lambda} \log S_w^* \quad (2a)$$

S_w	S_w^*	J	S_w	S_w^*	J
1.0	1.00	0.53	0.6	0.49	1.35
0.9	0.87	0.64	0.5	0.37	1.96
0.8	0.75	0.79	0.4	0.24	3.35
0.7	0.62	1.00	0.3	0.11	5.5

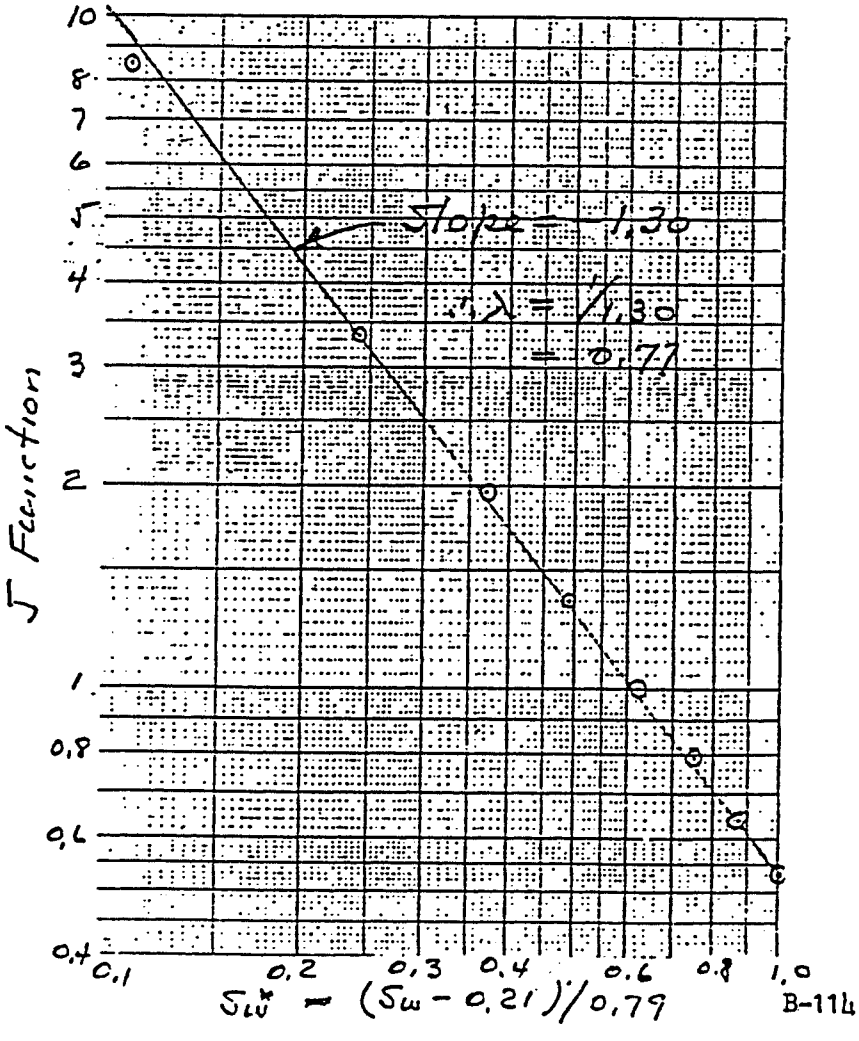

From plot of $\log J$ vs $\log S_w^*$

$\lambda = 0.77$

Solution Problem P-5 Cont

(2.) Calculation of k_{rg} & k_{ro} values. & plot.

From pg 25 of Fall Perm notes:

$$k_{rg}]_{dr} = \frac{k_g}{k} = k_r^o \left(\frac{S_g + S_{m-1}}{S_{m1} - S_{iw}} \right)^2 \left[1 - \left(1 - S_g^* \right)^{\frac{2+\lambda}{\lambda}} \right]$$

$$k_{ro}]_{dr} = \frac{k_o}{k} = k_r^o \left(S_o^* \right)^2 \left[\left(S_o^* + S_w^* \right)^{\frac{2+\lambda}{\lambda}} - \left(S_w^* \right)^{\frac{2+\lambda}{\lambda}} \right]$$

$k_r^o = 1.31 - 2.62(S_{iw}) + 1.1(S_{iw})^2 = 0.E0E$ (pg 14 Fall Pe

let $S_{m1} = 1$ $\quad S_w^* = \frac{0.296 - 0.210}{1 - 0.210} = 0.109$

S_g	S_L	$k_{rg}]_{dr}$	$k_{ro}]_{dr}$	S_g	S_L	$k_{rg}]_{dr}$	$k_{ro}]_{dr}$
6.0	1.0	0.000	0.642	0.4	0.6	0.191	0.0(
0.1	0.9	0.005	0.290	0.5	0.5	0.315	0.0(
0.2	0.8	0.034	0.115	0.6	0.4	0.463	5.(1(
0.3	0.7	0.096	0.035	0.7	0.3	0.634	—

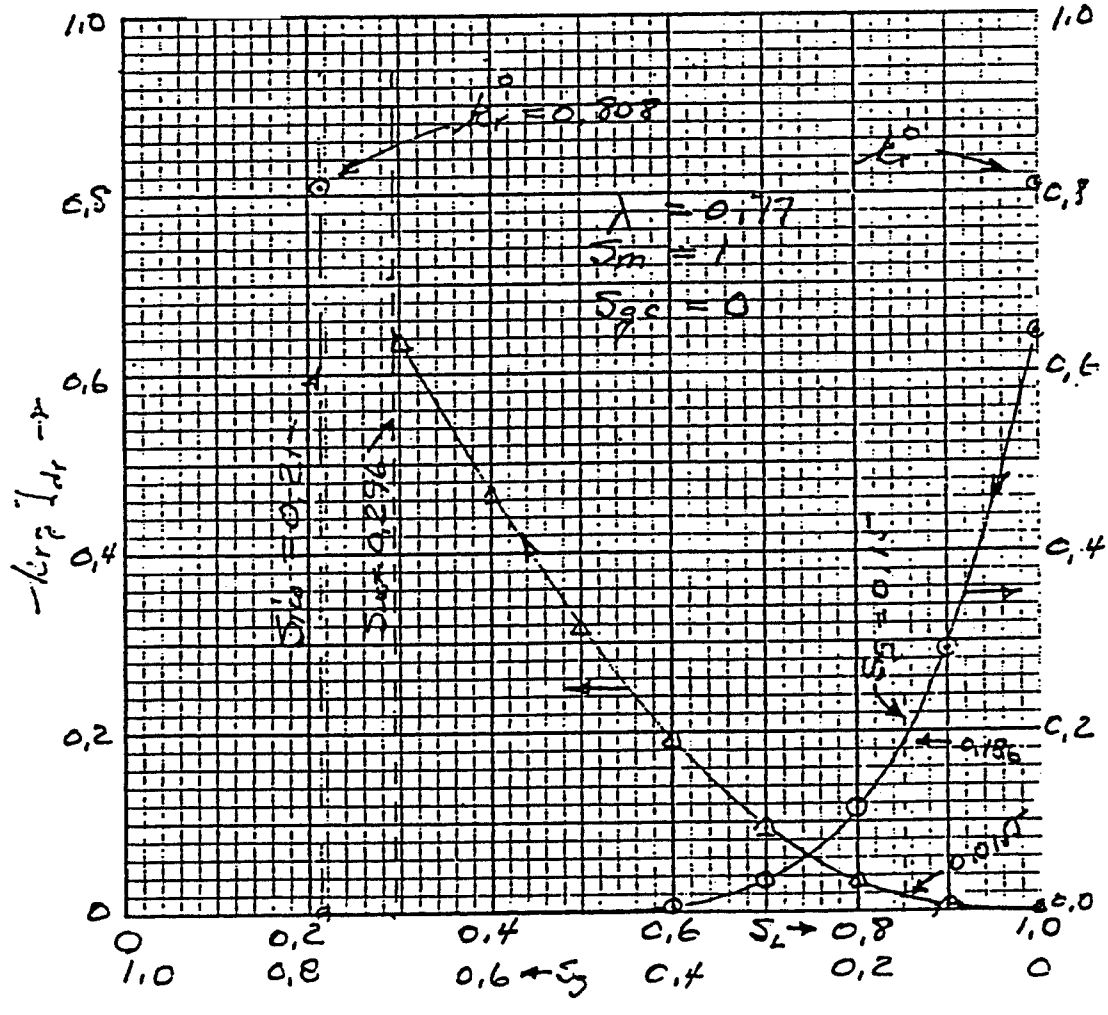

(4) Calc. (

$S_g = 0.1$

$k_g = k_{ro} \cdot k_r$

$= 816 \cdot 0.0$

$= 12.6$ mc

$k_o = E16 \cdot 0.1$

$= 15$ m

$k_w = (S_w^*)^{n}$

$= (0.109)^{n}$

$= 3.32$ (